

Matrix Integrals and the Generation and Counting of Virtual Tangles and Links

P. Zinn-Justin

*Laboratoire de Physique Théorique et Modèles Statistiques
Université Paris-Sud, Bâtiment 100
F-91405 Orsay Cedex, France*

and

J.-B. Zuber

*C.E.A.-Saclay, Service de Physique Théorique de Saclay,
CEA/DSM/SPhT, Unité de recherche associée au CNRS
F-91191 Gif sur Yvette Cedex, France*

Virtual links are generalizations of classical links that can be represented by links embedded in a “thickened” surface $\Sigma \times I$, product of a Riemann surface of genus h with an interval. In this paper, we show that virtual alternating links and tangles are naturally associated with the $1/N^2$ expansion of an integral over $N \times N$ complex matrices. We suggest that it is sufficient to count the equivalence classes of these diagrams modulo ordinary (planar) flypes. To test this hypothesis, we use an algorithm coding the corresponding Feynman diagrams by means of permutations that generates virtual diagrams up to 6 crossings and computes various invariants. Under this hypothesis, we use known results on matrix integrals to get the generating functions of virtual alternating tangles of genus 1 to 5 up to order 10 (i.e. 10 real crossings). The asymptotic behavior for n large of the numbers of links and tangles of genus h and with n crossings is also computed for $h = 1, 2, 3$ and conjectured for general h .

0. Introduction

Virtual knots have been introduced by Kauffman [1] as an extension of classical knots. They may be defined as equivalence classes of 4-valent (“4-regular”) diagrams with the ordinary under- or over-crossings of knot theory, plus a new type of *virtual* crossing, depicted with a small circle around the intersection, see fig. 1.



Fig. 1: Ordinary and virtual crossings

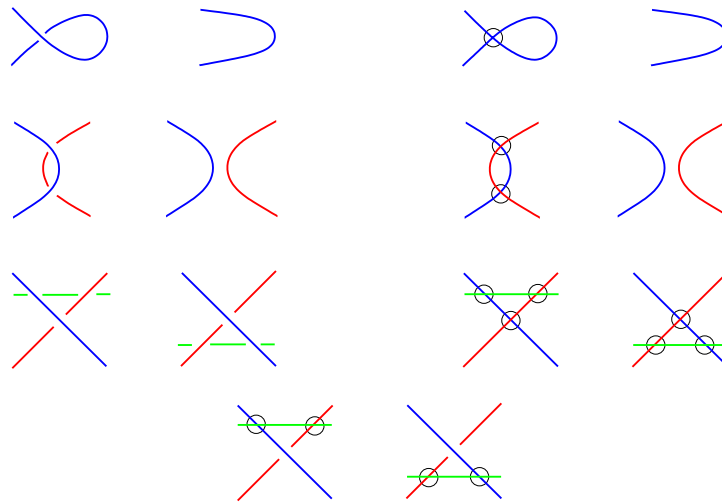


Fig. 2: Ordinary and virtual Reidemeister moves

Two such diagrams are equivalent if they may be connected by a sequence of generalized Reidemeister moves, see fig. 2. An example of a virtual link is provided by the following

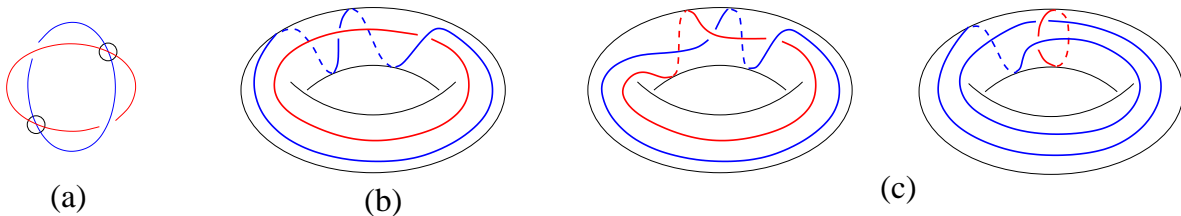


Fig. 3: A virtual link (a) in the previous notation; (b) as drawn on a genus 1 surface; (c) alternative representations, see below.

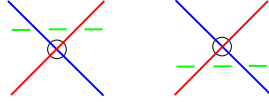


Fig. 4: A forbidden Reidemeister move

In this paper, we also use a different standpoint and notation, closer to graph theory: the ordinary crossings are regarded as vertices of a graph, the latter are regarded as rigid, i.e. the cyclic order of lines emanating from them cannot be changed, which essentially defines a (combinatorial) *map*, and the virtual crossings are artefacts forced in the planar representation by the connections between vertices. In this picture, the meaning of these new Reidemeister moves is clear: lines involving virtual crossings may be freely moved across the diagram, while keeping their end-points attached to vertices. Also natural in this picture is the impossibility for a virtual crossing to pass a line between two ordinary crossings, cf fig. 4.

Virtual knots (or links) may also be thought of as drawn in the vicinity of a connected compact orientable Riemann surface Σ of genus h , (h for “handles”), i.e. embedded into the “thickened” surface $\Sigma \times I$, with I an interval. The ordinary over-/under-crossings represent the projection of this knot on Σ , while the virtual ones represent the crossing of strands on different faces of Σ as seen in perspective. See fig. 3(b) for an example. To obtain virtual knots, we must consider equivalence classes of such embedded knots modulo isotopy in $\Sigma \times I$, and modulo orientation-preserving homeomorphisms of Σ , and addition or subtraction of empty handles, see [1,2]. This means that we are interested in virtual link diagrams as drawn on “abstract” Riemann surfaces, i.e. independently of the actual embedding and without any preferred choice of homology basis (See for example in Fig. 3(b)-(c) three equivalent representations of the virtual link (a) obtained from one another by various modular transformations). As we shall see, this is precisely what Feynman diagrams of a matrix integral do for us.

We shall use for virtual objects the same terminology of knots, links and tangles as for classical objects: a link has several connected components, while a knot has only one. Tangles, more precisely 4-tangles, have four open ends.

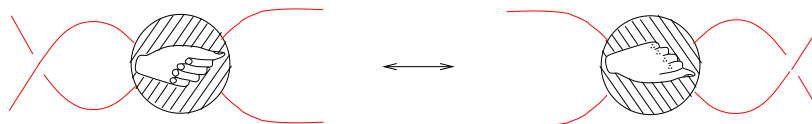


Fig. 5: The flype of a tangle

In the same way as *alternating* knots/links/tangles constitute an important subclass of the classical knotted objects, it is natural to define alternating virtual knots/links/tangles: they are simply described by diagrams of the previous type, with the condition that along any strand, one encounters alternatingly under- and over-crossings, ignoring possible virtual crossings. Of course, these diagrams have to be divided by the equivalence under Reidemeister moves or some combinations thereof. For classical alternating links/knots, it is a famous result, conjectured long ago by Tait and finally proved by Menasco and Thistlethwaite [3], that it is sufficient to consider *reduced* diagrams and act on them with *flypes*. Flypes are combinations of Reidemeister moves that preserve the alternating character, see fig. 5.

In a previous work [4], we have shown that the integral

$$Z_N(g, \alpha) = \int dM \exp -N \operatorname{tr} \left(\alpha M M^\dagger - \frac{g}{2} (M M^\dagger)^2 \right) . \quad (0.1)$$

over $N \times N$ complex matrices is well suited for the counting of alternating links and tangles: for an appropriate choice of $\alpha(g)$, see below, $2 \frac{\partial}{\partial g} \lim_{N \rightarrow \infty} \frac{1}{N^2} \log Z_N(g, \alpha(g))$ is the generating function of the numbers of alternating tangle diagrams with n 4-valent crossings, and eliminating the equivalence under the flypes just amounts to a “coupling constant renormalization” [5], as recalled below. In that way the results of [6] were reproduced.

It has been known to physicists since the pioneering work of 't Hooft [7] that the large N limit of the previous integral may be organized in a topological way. While the leading term corresponds to *planar* diagrams (in fact, drawn on a sphere), the subdominant terms of order N^{-2h} of $\frac{1}{N^2} \log Z(g)$ are described by graphs drawn on a Riemann surface of genus h . It is thus quite natural to expect that they will be in correspondence with virtual link diagrams, (or after differentiation with respect to g , with virtual tangle diagrams) and this is what we shall discuss and prove in the following.

This paper is organized as follows. We first recall (sect. 1) the dictionary between link/tangle diagrams and the “Feynman diagrams” of the matrix integral (0.1), and the necessary steps to eliminate the redundancy in the counting. First remove spurious diagrams, non-prime or “nugatory” in the knot terminology, by a suitable choice of the function $\alpha(g)$. Then we must address the burning question of eliminating the remaining redundancies. We argue – but this remains a heuristic argument – that the same (planar) flypes as for classical alternating links and tangles are still sufficient to remove the redundancies of alternating virtual diagrams. We call this the “generalized flype conjecture” and

defer until sect. 4 arguments in favor of this conjecture. The flypes are taken into account by a redefinition (“renormalization”) of the coupling constant: $g \rightarrow g_0(g)$. In sect. 2 we apply these ideas to the case $N = 1$, which corresponds to the enumeration irrespective of the genus; this serves as a sum rule in what follows. In sect. 3 the explicit expressions of the first four terms in the large N expansion of $F(g, N)$ are presented, corresponding to genus $h = 0, 1, 2$ and 3 respectively: while the leading term is well known (and has been used in [4]) and the second one ($h = 1$) has been derived by Morris [8], the genus 2 and 3 contributions computed by Akemann and by Adamietz [9,10] from the work of [11] may be less known. Using the results of previous section and computing the lowest contributions of a given genus (Appendix A) gives us enough information to completely determine the numbers of all virtual diagrams up to 11 crossings for the links, or 10 for the tangles, and up to genus 5. We also give tables of virtual alternating links up to four (real) crossings. The rate of growth of the number of virtual diagrams of genus 1, 2 and 3 is also derived from these expressions, and a general Ansatz is proposed for generic h , following what is regarded as standard lore by physicists. Using the generalized flyping conjecture, we then obtain the generating functions of virtual alternating 4-tangles for genus 0 to 3. Their asymptotic behaviors for large number of (real) crossing are, up to a larger radius of convergence, the same as the previous ones, and under the very plausible assumption (proved in [12] for classical links) that generic links have no symmetry, we can also estimate the asymptotic number of virtual alternating links of a given genus.

Finally, in sect. 4, we recall that there exists a way to encode the relevant Feynman diagrams by means of permutations. This is presumably an old idea; in the present context, it seems to be due to Drouffe, it was used in [13], and more recently in related topics by combinatorialists [14-15]. Here we use it to set up an algorithm which is able to build all virtual link/tangle diagrams (up to six/five crossings). We have used this to test the “generalized flype conjecture” by constructing as many invariants as possible, to make sure that the objects that cannot be obtained by flypes from each other are indeed topologically distinct. We provide samples of the data thus produced (the full output being accessible on the web: <http://ipnweb.in2p3.fr/~lptms/membres/pzinn/virtlinks>), and discuss the conclusions one can draw from them.

1. Matrix integrals and virtual links

1.1. Feynman rules for matrix integrals

We first recall the diagrammatic techniques to derive a series expansion in g of the integral (0.1): see [13,16] for a general introduction and [4] for a discussion in the present context. The integration measure in (0.1) is

$$dM = \prod_{1 \leq i, j \leq N} d\Re e M_{ij} d\Im m M_{ij} . \quad (1.1)$$

We shall be mostly interested in the “free energy”


$$F(g, \alpha) = \lim_{N \rightarrow \infty} \frac{1}{N^2} \log \frac{Z(\alpha, g)}{Z(\alpha, 0)} \quad (1.2)$$

and its derivatives. The constant α can be absorbed in a rescaling $M \rightarrow \alpha^{-\frac{1}{2}} M$:

$$Z(g, \alpha) = \alpha^{-\frac{N^2}{2}} Z\left(\frac{g}{\alpha^2}, 1\right) \quad (1.3a)$$

$$F(g, \alpha) = F\left(\frac{g}{\alpha^2}, 1\right) \quad (1.3b)$$

but it is useful to keep it.

Define the “propagator” as the inverse of the quadratic form in (0.1), represented as $j \begin{array}{c} \leftarrow \\ \rightleftarrows \\ \rightarrow \end{array} k = \frac{1}{N\alpha} \delta_{il} \delta_{jk}$ and the 4-vertex as the tensor  $= gN \delta_{qi} \delta_{jk} \delta_{lm} \delta_{np}$. This four-vertex is to be considered as a rigid crossing, which cannot be flipped and in which the cyclic order of the lines cannot be changed. In both the propagator and the 4-vertex, the small arrows distinguish the row and column indices of the matrices, while the wide one distinguishes M from M^\dagger .

The prescriptions to compute the n -th order of the g -expansion of F , known as Feynman rules, are as follows: draw n four-vertices, then draw all the topologically distinct connected graphs obtained by joining by propagators the double lines emerging from these n 4-vertices, while respecting the orientations, and sum over the matrix indices $i, j, \dots = 1, \dots, N$. Each graph then comes with a weight $g^n N^\# / \alpha^{2n}$, where the power of N will be computed below, and a “symmetry factor”, which is the inverse of the order of the group of permutations of the lines and vertices which leave the structure of the graph unchanged (see below an alternative characterization of this factor).

When drawing these Feynman diagrams on a plane, one usually encounters topological obstructions which force one to introduce additional crossings (over- or under-, it is immaterial). Alternatively, these diagrams may be drawn on a higher genus Riemann surface

as can be seen as follows. The identification of matrix indices by the Kronecker delta's of the propagators and 4-vertices leaves us with a number $\#F$ of index loops. By pasting a domain homeomorphic to a disk to each such loop, we build a discretized Riemann surface with n edges, $2n$ edges and $\#F$ faces.

Thus Feynman diagrams for $F(g, \alpha)$ may be regarded as discretized orientable Riemann surfaces Σ . Their faces are oriented by the small arrows carried by the propagators. In addition their edges carry the orientation of the big arrows. According to the argument of 't Hooft [7] and following the rules above, if a diagram has $\#V = n$ vertices, hence $\#E = 2n$ edges (propagators), and $\#F$ faces, it carries a power of N equal to $n - 2n + \#F = \chi_E(\Sigma) = 2 - 2h$, the Euler-Poincaré characteristics expressed in terms of the genus h .

To summarize, we have obtained a topological expansion (which is an asymptotic expansion in $1/N^2$)

$$F(g, \alpha) = \sum_{h=0}^{\infty} \frac{1}{N^{2h}} F^{(h)}(g, \alpha) \quad (1.4)$$

where $F^{(h)}$ is the sum over Feynman diagrams of genus h weighed as explained above. Now that this property has been established, we abandon the double line notation and return to more conventional notations for Feynman diagrams: we erase the small arrows of matrix indices but retain the big ones that encode the distinction between M and M^\dagger .

We are now ready to build a dictionary with virtual links: due to the “contraction” of M and M^\dagger through the propagators, Feynman diagrams of the type just discussed are naturally endowed with the properties of alternating virtual link diagrams. Thus 4-vertices are in one-to-one correspondence with over/under-crossings $\begin{array}{c} \diagup \\ \diagdown \end{array} \Leftrightarrow \begin{array}{c} \diagdown \\ \diagup \end{array}$, while the virtual crossings admit the alternative representation: $\begin{array}{c} \diagup \\ \diagdown \end{array} = \begin{array}{c} \diagdown \\ \diagup \end{array} \Leftrightarrow \begin{array}{c} \diagdown \\ \diagup \end{array}$. (Beware! a virtual crossing is depicted in the graph theoretic way as an under- or over-crossing in the Feynman diagram representation; as mentioned above, it is immaterial to draw it either way.) Note that in this representation, it is quite natural that these virtual crossings can be freely moved around, thus enforcing the virtual Reidemeister moves. Note also that this correspondence gives an operative way to compute the genus on which to draw a given virtual link diagram, which may not have been obvious in their original presentation (whether or not this is the *minimal* genus on which one can draw the link itself is a subtle matter due to the existence of the “real” Reidemeister moves, and it will be discussed again in section 4).

From the relations $n = \#F + 2h - 2$ and $\#F \geq 1$, we might have expected contributions of genus h to occur first at order $n = 2h - 1$, for diagrams with a single face. This is indeed what happens with diagrams related to hermitian matrix integrals. Here, however, the orientation of edges by the big arrows induces an additional constraint: adjacent faces have opposite orientations with respect to these arrows. This forbids the possibility to have $\#F = 1$ and as a result, genus $h > 0$ occurs first at order

$$n_{\min}(h) = 2h , \quad (1.5)$$

i.e. $F^{(h)}(g, \alpha)$ starts at order g^{2h} , or said otherwise, there is no virtual link of genus h with less than $2h$ (real) crossings. One checks that the bound is saturated by computing the coefficient,

$$F_{2h}^{(h)} = \frac{(4h - 1)!!}{4h(2h + 1)} . \quad (1.6)$$

and it is also possible to determine without much further effort the next term, i.e. the coefficient of g^{2h+1}

$$F_{2h+1}^{(h)} = \frac{(4h + 1)!!}{(2h + 1)^2} \sum_{s=0}^{2h} \frac{(-1)^{\lfloor \frac{s+1}{2} \rfloor}}{\binom{4h+1}{s}} \binom{2h}{\lfloor \frac{s}{2} \rfloor} \sum_{p=s+1}^{4h+1-s} \frac{1}{p} , \quad (1.7)$$

see Appendix A for details.

1.2. Correlation functions

We are also interested in the “ $2p$ -point functions” $G_{2p}(g, \alpha) := \langle \frac{1}{N} \text{tr}(MM^\dagger)^p \rangle$, in particular

$$G_4(g, \alpha) = 2 \frac{\partial F(g, \alpha)}{\partial g} \quad (1.8)$$

and

$$G_2(g, \alpha) = \frac{1}{\alpha} - \frac{\partial}{\partial \alpha} F(g, \alpha) = \frac{1}{\alpha} (1 + gG_4) , \quad (1.9)$$

where use has been made of the homogeneity property (1.3). This same property implies that

$$\begin{aligned} G_{2p}(g, \alpha) &= \frac{1}{\alpha^p} G_{2p} \left(\frac{g}{\alpha^2} \right) \\ G_{2p}(g) &:= G_{2p}(g, 1) \end{aligned} \quad (1.10)$$

These functions too admit a graphical representation, with similar Feynman rules and Feynman graphs with $2p$ external lines. These graphs are natural candidates for $2p$ -tangle diagrams. For the four-point function G_4 , we adopt the following convention of orientation: external lines may be extended to a circle surrounding the diagram, and the four lines are drawn in the NW, NE, SE and SW directions, with the outgoing arrow (i.e. first crossing is over-) on NW and SE external lines.

1.3. Nugatory crossings and non-prime diagrams

The two-point function G_2 is in particular useful to dispose of all composite links and tangles. Irrelevant “nugatory” crossings and non prime diagrams appear as graphs with a subgraph which may be disconnected by cutting transversely two distinct edges. Such a subgraph is called a “self-energy” by physicists. To remove all nugatory crossings and non prime configurations, i.e. to retain only diagrams with no self-energy, it suffices to choose $\alpha = \alpha(g)$ so as to make $G_2(g, \alpha(g)) = 1$ or equivalently in view of (1.10), $G_2(g/\alpha(g)^2) = \alpha$, and to plug it into $F(g, \alpha)$ or $G_{2p}(g, \alpha)$. Then the “connected four-point function with no self-energy” defined as

$$\Gamma(g) = G_4(g, \alpha(g)) - 2 \tag{1.11}$$

is easily seen to satisfy

$$g\Gamma(g) = \alpha(g) - 1 - 2g \tag{1.12}$$

as a consequence of (1.9). (The appearance of -2 in (1.11) is due to the subtraction of disconnected contributions to the 4-tangle by two parallel non-intersecting strands.)

1.4. Flypes

We now want to argue that dividing only by the *planar* flypes suffices to get the equivalence classes of virtual alternating tangles and links. This claim is based partially on our intuition that other types of moves, such as flypes of higher genus, are not permitted by the structure of the thickened surface, and partially on the study of low order virtual links and tangles. But our best evidence comes from the analysis, explained in section 4, of several classes of invariants applied to links and tangles up to order 6 (six real crossings), which indicates that the remaining objects are indeed topologically inequivalent. Still this remains an assumption. . .

For classical (genus 0) tangles, Sundberg and Thistlethwaite have shown how to construct the generating function of flype-equivalence classes of tangles $\tilde{\Gamma}^{(0)}(g)$ from the planar generating function $\Gamma^{(0)}(g) \equiv \lim_{N \rightarrow \infty} \Gamma(g)$ [6]. The operations leading from $\Gamma^{(0)}(g)$ to $\tilde{\Gamma}^{(0)}(g)$ have subsequently been shown by one of us [5] to be simply expressible in terms of a “coupling constant renormalization” in the language of physicists, i.e. of a redefinition of the expansion variable, determined in a self-consistent way. Let $g_0(g)$ be the solution of

$$g_0 = g \left(-1 + \frac{2}{(1-g)(1+\Gamma^{(0)}(g_0))} \right) . \tag{1.13}$$

Then we recover the result of Sundberg and Thistlethwaite by writing that $\tilde{\Gamma}^{(0)}(g) = \Gamma^{(0)}(g_0(g))$. According to our conjecture, we must generalize this to all genera. If $\tilde{\Gamma}(g) = \sum_{h=0}^{\infty} N^{-2h} \tilde{\Gamma}^{(h)}(g)$ is the full generating function of virtual prime alternating tangles, then we are led to

$$\tilde{\Gamma}(g) = \Gamma(g_0(g)) . \quad (1.14)$$

2. Sum over all genera

For $N = 1$ the integral over a single real variable is readily computed. One finds for Z the asymptotic expansion

$$Z(g, \alpha = 1)|_{N=1} = \sum_0^{\infty} \left(\frac{g}{2}\right)^n \frac{(2n)!}{n!} . \quad (2.1)$$

Its logarithm

$$\begin{aligned} F(g, \alpha = 1)|_{N=1} = & g + \frac{5}{2} g^2 + \frac{37}{3} g^3 + \frac{353}{4} g^4 + \frac{4081}{5} g^5 + \frac{55205 g^6}{6} g^6 + \frac{854197}{7} g^7 \\ & + \frac{14876033}{8} g^8 + \frac{288018721}{9} g^9 + \frac{1227782785}{2} g^{10} + \frac{142882295557}{11} g^{11} + O(g^{12}) \end{aligned} \quad (2.2)$$

is the sum of $F^{(h)}$ for all genera h and will provide a sum rule over the contributions of the different genera to be discussed in the next section. By differentiation one gets the 4-point function

$$\begin{aligned} G_4(g) = & 2 + 10 g + 74 g^2 + 706 g^3 + 8162 g^4 + 110410 g^5 + 1708394 g^6 \\ & + 29752066 g^7 + 576037442 g^8 + 12277827850 g^9 + 285764591114 g^{10} + O(g^{11}) \end{aligned} \quad (2.3)$$

and after determination of $\alpha(g)$ as explained in sect. 1.3, one gets the connected four-point function with no self-energy

$$\begin{aligned} \Gamma(g) = & 2 g + 10 g^2 + 82 g^3 + 898 g^4 + 12018 g^5 + 187626 g^6 \\ & + 3323682 g^7 + 65607682 g^8 + 1424967394 g^9 + 33736908874 g^{10} + O(g^{11}) . \end{aligned} \quad (2.4)$$

Expanding Eq. (1.13) to the required order, we find

$$g_0 = g - 2 g^3 - 4 g^4 - 10 g^5 - 30 g^6 - 108 g^7 - 436 g^8 - 1890 g^9 - 8588 g^{10} + O(g^{11}) \quad (2.5)$$

and therefore

$$\begin{aligned} \tilde{\Gamma}(g) = & 2 g + 10 g^2 + 78 g^3 + 850 g^4 + 11426 g^5 + 179238 g^6 \\ & + 3187002 g^7 + 63095526 g^8 + 1373767142 g^9 + 3259401885 g^{10} + O(g^{11}) . \end{aligned} \quad (2.6)$$

The three expansions $G_4(g)$, $\Gamma(g)$ and $\tilde{\Gamma}(g)$ have the same asymptotic behavior up to a multiplicative constant, with their n -th order of the form $\text{const. } 2^n \sqrt{n+1} (n+1)!$

3. Genus 0, 1, 2 and 3

We now return to the matrix integral (0.1) and its $1/N^2$ expansion. Let $a^2(g)$ be the solution of

$$a^2 = 1 + 3g(a^2)^2 \quad (3.1)$$

with $a^2(g) = 1 + O(g)$. (Its interpretation is that it characterizes the support of the limiting distribution of eigenvalues of MM^\dagger .) Then one finds

$$\begin{aligned} F^{(0)}(g) &:= F^{(0)}(g, 1) = \log a^2 - \frac{1}{12}(a^2 - 1)(9 - a^2) \\ &= 2 \sum_{n=1}^{\infty} (3g)^n \frac{(2n-1)!!}{n!(n+2)!} \end{aligned}$$

(As a side-remark, we recall that this is twice the result for the Hermitian matrix integral as in (0.1) but with $\text{tr} \left(\frac{\alpha}{2} M^2 - \frac{g}{4} M^4 \right)$ in the exponential). Explicitly, one gets the expansion

$$\begin{aligned} F^{(0)}(g) &= g + \frac{9}{4} g^2 + 9 g^3 + \frac{189}{4} g^4 + \frac{1458}{5} g^5 + \frac{8019}{4} g^6 + \frac{104247}{7} g^7 \\ &\quad + \frac{938223}{8} g^8 + 966654 g^9 + \frac{82648917}{10} g^{10} + \frac{801058734}{11} g^{11} + O(g^{12}). \end{aligned} \quad (3.3)$$

For genus 1, Morris gives [8]

$$\begin{aligned} F^{(1)}(g) &= -\frac{1}{24} \log \frac{(2-a^2)(2+a^2)^3}{27} \\ &= \frac{1}{24} \sum_{n=0}^{\infty} \frac{(3g)^{n+1}}{n+1} \sum_{p=0}^n \frac{(2n+2)!}{(n-p)!(n+2+p)!} (1 - (-3)^{-p}) \\ &= \frac{1}{4} g^2 + \frac{10}{3} g^3 + \frac{307}{8} g^4 + 428 g^5 + \frac{28457}{6} g^6 + 52612 g^7 + \frac{9370183}{16} g^8 \\ &\quad + \frac{58911256}{9} g^9 + \frac{734641583}{10} g^{10} + 827733428 g^{11} + O(g^{12}). \end{aligned}$$

For higher genus, the expressions are more and more complicated. Akemann and Adamietz [9,10] have found that in terms of $I_1 = 1 - 6ga^2$ and $M_0 = 1 - 2ga^2$

$$\begin{aligned} F^{(2)}(g) &= \frac{21a^2g^3}{40I_1^5} - \frac{69g^2}{640I_1^4} + \frac{53g}{2560a^2I_1^3} + \frac{g}{256a^2I_1^2M_0} \\ &\quad - \frac{3g}{512a^2M_0^3} - \frac{1}{512a^4I_1M_0} - \frac{3}{1024a^4M_0^2} - \frac{53}{15360a^4I_1^2} \end{aligned}$$

whence

$$\begin{aligned} F^{(2)}(g) &= \frac{21}{8} g^4 + \frac{483}{5} g^5 + \frac{4659}{2} g^6 + 46434 g^7 \\ &\quad + \frac{6635991}{8} g^8 + 13798410 g^9 + \frac{1091610282}{5} g^{10} + 3328687092 g^{11} + O(g^{12}) \end{aligned} \quad (3.6)$$

and the expression of $F^{(3)}(g)$ is too cumbersome to be given here but leads to the expansion

$$F^{(3)}(g) = \frac{495}{4} g^6 + \frac{56628}{7} g^7 + \frac{2504115}{8} g^8 + 9322668 g^9 + \frac{472138479}{2} g^{10} + 5345163216 g^{11} + O(g^{12}) . \quad (3.7)$$

We check that these $F^{(h)}$ start at an order in g consistent with (1.5). Moreover the sum of these four first contributions differ from the sum over all genera (2.2) by terms of order g^8 as it should. Using the additional information of (1.6) and (1.7), one may extract the first terms of $F^{(4)}$ and $F^{(5)}$

$$\begin{aligned} F^{(4)} &= \frac{2252225}{16} g^8 + 1368653 g^9 + \frac{1495900107}{20} g^{10} + 3023618067 g^{11} + O(g^{12}) \\ F^{(5)} &= \frac{11904165}{4} g^{10} + \frac{4304016990}{11} g^{11} + O(g^{12}) . \end{aligned} \quad (3.8)$$

By differentiating with respect to g , one gets $G_2^{(h)}(g, 1)$ and $G_4^{(h)}(g, 1)$ according to (1.9) and (1.8). One then determines the double expansion in powers of g and $1/N^2$ of $\alpha(g)$ so as to remove the self-energies, as explained at the end of sect. 1. We don't display the corresponding expansion of $\alpha(g)$ as it may be recovered from eqn (1.12) and the expressions of $\Gamma^{(h)}$ below. Using the additional data of (3.8) we may provide the g -expansion up to order g^{10} of $\Gamma^{(h)}(g)$ for $h = 0, \dots, 5$.

$$\begin{aligned} \Gamma^{(0)}(g) &= g + 2g^2 + 6g^3 + 22g^4 + 91g^5 + 408g^6 + 1938g^7 + 9614g^8 + 49335g^9 + 260130g^{10} + O(g^{11}) \\ \Gamma^{(1)}(g) &= g + 8g^2 + 59g^3 + 420g^4 + 2940g^5 + 20384g^6 + 140479g^7 + 964184g^8 + 6598481g^9 + 45059872g^{10} + O(g^{11}) \\ \Gamma^{(2)}(g) &= 17g^3 + 456g^4 + 7728g^5 + 104762g^6 + 1240518g^7 + 13406796g^8 + 135637190g^9 + 1305368592g^{10} + O(g^{11}) \\ \Gamma^{(3)}(g) &= 1259g^5 + 62072g^6 + 1740158g^7 + 36316872g^8 + 627368680g^9 + 9484251920g^{10} + O(g^{11}) \\ \Gamma^{(4)}(g) &= 200589g^7 + 14910216g^8 + 600547192g^9 + 17347802824g^{10} + O(g^{11}) \\ \Gamma^{(5)}(g) &= 54766516g^9 + 5554165536g^{10} + O(g^{11}) \end{aligned} \quad (3.9)$$

are the generating functions of the numbers of connected graphs of genus 0 to 3 with no self-energy; they are not yet the generating functions of the number of tangle diagrams, due to the flype equivalence and possible other redundancies. One may integrate these expressions according to (1.8) to obtain the corresponding generating functions $F^{(h)}(g)$ of virtual alternating link diagrams with no self-energy.

In figures 6-10 we depict the corresponding diagrams of $F^{(h)}$, $h = 0, 1, 2$ up to order 4: the corresponding diagrams of Γ are obtained by removing in all possible non equivalent ways one vertex, thus opening the link diagram into a tangle. In these figures, we list in

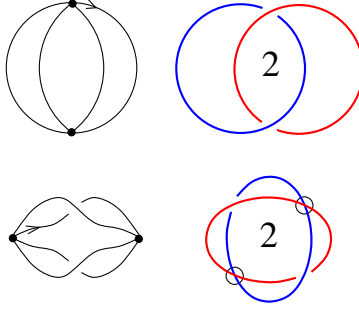


Fig. 6: The genus 0 and 1 2-crossing alternating virtual link diagrams in the two representations, the Feynman diagrams on the left, the virtual diagrams on the right: for each, the inverse of the weight in F is indicated

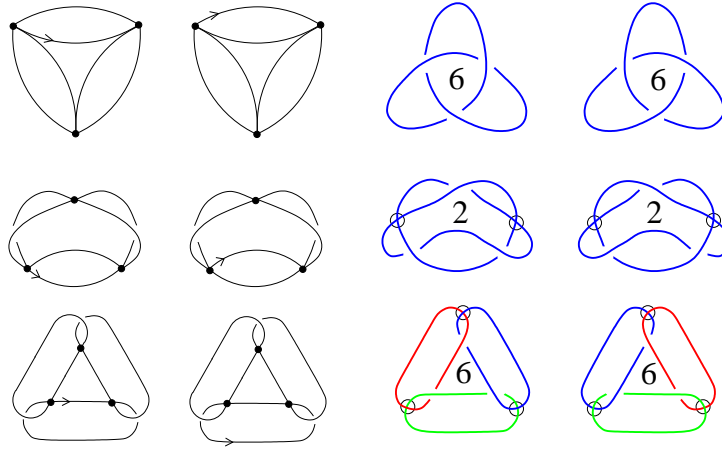


Fig. 7: same for order 3, genus 0 and 1

parallel the two notations of Feynman diagrams and of links. In the latter, colors have been introduced only to distinguish the different connected components. Each link of order n (n crossings) comes with an integer, whose inverse gives its weight in $F^{(h)}$. Alternatively, the number of distinct contributions that this link gives to $\Gamma^{(h)}$ after removal of one vertex equals $2n$ divided by this integer.

The first flypes occur at order 3 for genus 0 or genus 1 in Γ , see fig. 11. The generating functions of flype equivalence classes of classical links is

$$\tilde{\Gamma}^{(0)}(g) = \Gamma^{(0)}(g_0) = g + 2g^2 + 4g^3 + 10g^4 + 29g^5 + 98g^6 + 372g^7 + 1538g^8 + 6755g^9 + 30996g^{10} + O(g^{11})$$

(which is the result of [6]). Then, according to our assumption,

$$\begin{aligned} \tilde{\Gamma}^{(1)}(g) = \Gamma^{(1)}(g_0) = & g + 8g^2 + 57g^3 + 384g^4 + 2512g^5 \\ & + 16158g^6 + 102837g^7 + 649862g^8 + 4086137g^9 + 25597900g^{10} + O(g^{11}) \end{aligned}$$

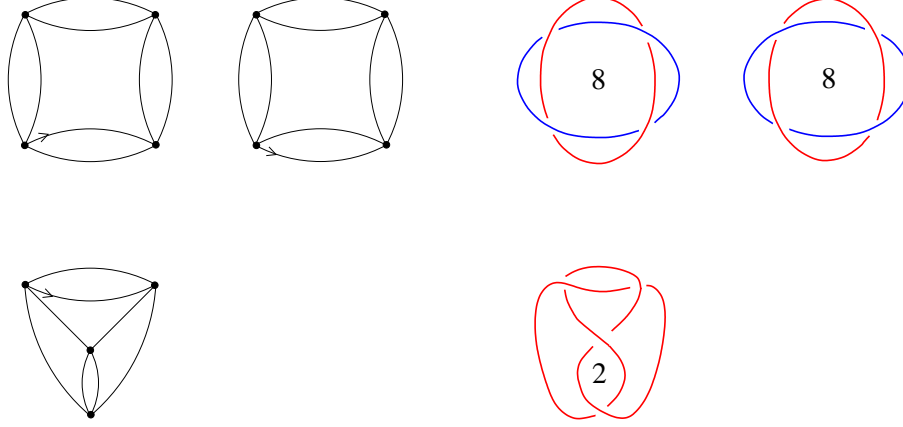


Fig. 8: same for order 4, genus 0

$$\begin{aligned} \tilde{\Gamma}^{(2)}(g) = \Gamma^{(2)}(g_0) = & 17g^3 + 456g^4 + 7626g^5 + 100910g^6 + 1155636g^7 + 11987082g^8 \\ & + 115664638g^9 + 1056131412g^{10} + O(g^{11}) \end{aligned}$$

$$\begin{aligned} \tilde{\Gamma}^{(3)}(g) = \Gamma^{(3)}(g_0) = & 1259g^5 + 62072g^6 + 1727568g^7 + 35546828g^8 + 601504150g^9 \\ & + 8854470134g^{10} + O(g^{11}) \end{aligned} \quad (3.10)$$

$$\tilde{\Gamma}^{(4)}(g) = \Gamma^{(4)}(g_0) = 200589g^7 + 14910216g^8 + 597738946g^9 + 17103622876g^{10} + O(g^{11})$$

$$\tilde{\Gamma}^{(5)}(g) = \Gamma^{(5)}(g_0) = 54766516g^9 + 5554165536g^{10} + O(g^{11})$$

are the generating functions of flype-equivalence classes of virtual tangles with up to 10 real crossings. For example, the reduction from 59 to 57 of the number of genus 1 tangles of order 3 is in accordance with the equivalence of fig. 11.

The large order behavior of the g -expansions of $F^{(h)}$ is dominated by the leading singularity of $a^2(g)$, which occurs at $g = g_c = 1/12$, $a^2(g_c) = 2$. One finds

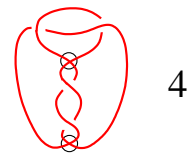
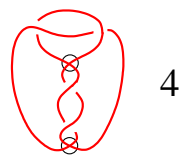
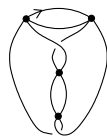
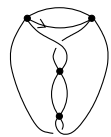
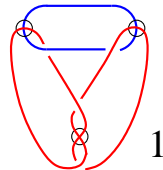
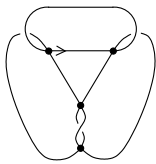
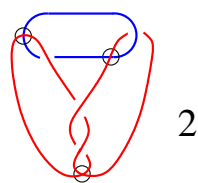
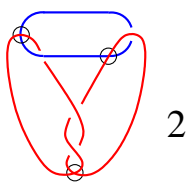
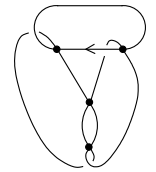
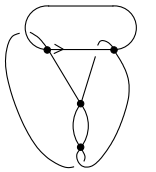
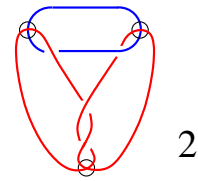
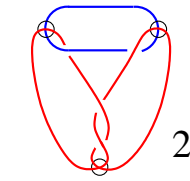
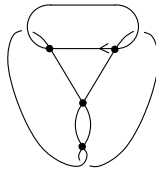
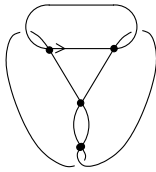
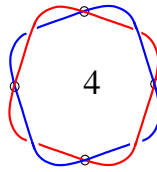
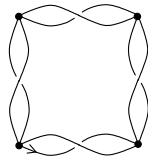
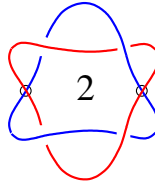
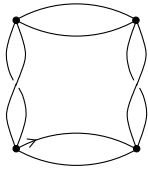
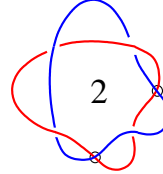
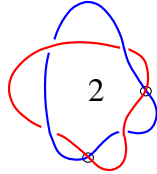
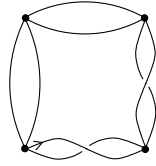
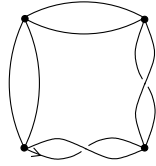
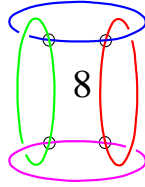
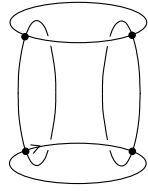
$$\begin{aligned} F^{(0)}(g, 1) &\approx (g_c - g)^{5/2} \\ F^{(1)}(g, 1) &\approx \log(g_c - g) . \end{aligned} \quad (3.11)$$

The leading singularity of the expression of $F^{(2)}$ comes from the term proportional to I_1^{-5} , as I_1 vanishes like $(g_c - g)^{1/2}$. Similarly $F^{(3)}$ has a pole of order 10 in I_1 . This is typical of what is expected for generic genus [17]

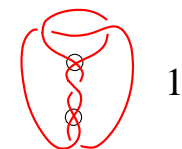
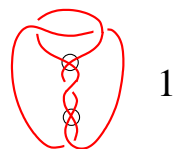
$$F^{(h)}(g) \approx (g_c - g)^{5/2(1-h)} . \quad (3.12)$$

Thus one expects

$$f_n^{(h)} \approx \frac{1}{g_c^n} n^{5/2(h-1)-1} , \quad (3.13)$$



14



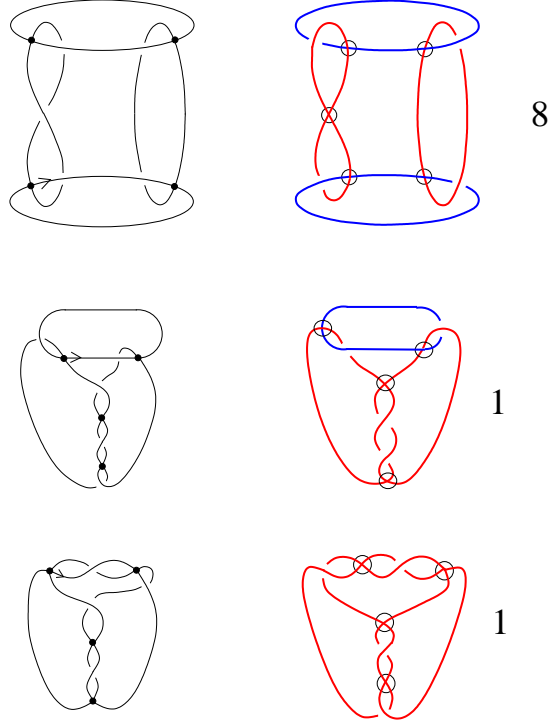


Fig. 10: *ibid* for genus 2

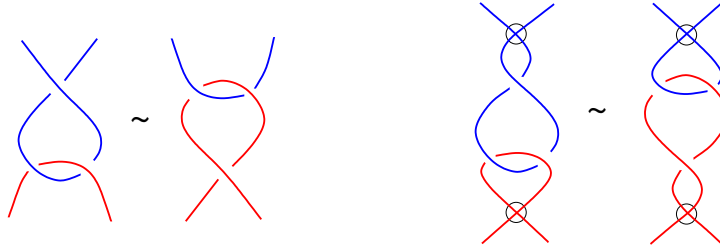


Fig. 11: First occurrences of flype equivalence in tangles with 3 crossings

and correspondingly, for $\Gamma^{(h)}(g) = \sum_n \gamma_n^{(h)} g^n$

$$\gamma_n^{(h)} \approx \frac{1}{g_c^n} n^{5/2(h-1)}. \quad (3.14)$$

The subsequent reductions that we perform to eliminate the redundancies, change the value of g_c (enlarging it so as to increase the radius of convergence) but do not affect the value of the “critical exponents” $5/2, 0, -5/2, \dots$. Thus, removing the self-energies has the effect that the closest singularity is now for $g/\alpha^2(g) = 1/12$ which gives [4] $g'_c = 4/27$. Similarly, taking care of the flype equivalence increases the radius of convergence of $\tilde{\Gamma}(g)$ to the value $g''_c = (-101 + \sqrt{21001})/270$, see [6], but does not affect the general form (3.14).

Finally, note that the function $\tilde{F}(g)$ obtained by integrating $\tilde{\Gamma}$ is not exactly the generating function of flype-equivalence classes of links (due to the issue of symmetry factors) but should have the same asymptotic behavior: intuitively, this reflects the fact that the number of link diagrams with a non trivial symmetry factor is subleading and does not contribute to the asymptotic behavior of the form (3.13) (this fact has now been proved for classical links [12]).

4. An algorithm to classify virtual alternating links

In this section we describe the encoding we used to represent virtual alternating link diagrams, and the subsequent algorithm that allowed us to generate prime alternating virtual links. Due to the factorial growth of their number, we only describe the result up at order 4; but we have obtained data up to order 6 in order to check our generalized flype conjecture.

4.1. Alternating link diagrams and permutations

Our encoding of virtual alternating link diagrams is based on a well-known correspondence between bicolored maps and permutations. An alternating link diagram can be equivalently described as a (not necessarily planar) map whose vertices have valence 4 and whose faces are bicolored, according to the pattern of under/over crossings as one moves around the face, see Fig. 12.

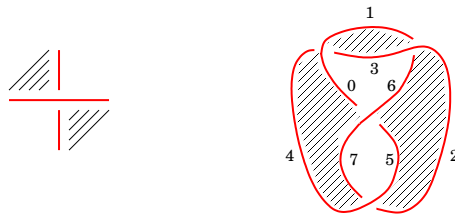


Fig. 12: Bicoloration and labelling of an alternating link diagram.

Let us now *label* the edges of the diagram (or of the map): the set of edge labels will be called E , and its permutation group $\mathcal{S}(E)$. In the implementation, E is chosen to be $E = \{0, 1, \dots, 2n - 1\}$. It is known that general face-bicolored maps (i.e. duals of bipartite maps) are in one-to-one correspondence to pairs of permutations $(\sigma, \tau) \in \mathcal{S}(E)$ according to the following recipe: the cycles of σ (resp. τ) are the labels of the edges in their cyclic order as one turns clockwise around white faces (resp. counterclockwise around

black faces).¹ Define additionally $\rho = \sigma^{-1}\tau$ and $\tilde{\rho} = \sigma\tau^{-1}$. The cycles of ρ (or of $\tilde{\rho}$) are easily seen to be in one-to-one correspondence with vertices of the map.

Finally a relabelling of the map is a permutation $g \in \mathcal{S}(E)$ of the labels acting by conjugation:

$$\sigma' = g\sigma g^{-1} \quad \tau' = g\tau g^{-1} \quad (4.1)$$

An unlabelled map can therefore be described as a conjugacy class of pairs of permutations.

Here we require various additional properties of the map, which must be translated combinatorially into properties of the permutations:

1) First and foremost, all vertices must have valence 4. This implies that ρ (resp. $\tilde{\rho}$) only has 2-cycles, i.e. is a fixed point-free involution, exchanging edges at overcrossings (resp. undercrossings). Here we decide to focus on ρ rather than $\tilde{\rho}$. The situation at each vertex is described on Fig. 13; the figure can be considered as the defining rule to build σ and τ .

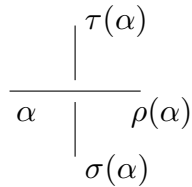


Fig. 13: Configuration at a vertex. If $\beta = \rho(\alpha)$, consistency implies that $\sigma(\alpha) = \tau(\beta)$ and $\tau(\alpha) = \sigma(\beta)$ i.e. that $\rho = \tau^{-1}\sigma = \sigma^{-1}\tau$ is an involution.

One can partially fix the freedom on the labels by noting that via conjugations, one can reduce ρ to a given form; for $E = \{0, 1, \dots, 2n - 1\}$, we choose

$$\rho(2\alpha) = 2\alpha + 1 \quad \rho(2\alpha + 1) = 2\alpha \quad \alpha = 0, \dots, n - 1 \quad (4.2)$$

Once ρ is fixed, the data of σ alone suffices to describe the alternating link diagram since $\tau = \sigma\rho$. Furthermore, all relabellings must commute with ρ ; they form a group $G = \{g \in \mathcal{S}(E) \mid g\rho = \rho g\}$ which is isomorphic to $\mathcal{S}_n \times \mathbb{Z}_2^n$.

For example, the labelled diagram of Fig. 12 is such that ρ is of the form of Eq. (4.2), and we find

$$\sigma = \begin{pmatrix} 0 & 1 & 2 & 3 & 4 & 5 & 6 & 7 \\ 3 & 4 & 1 & 6 & 2 & 7 & 0 & 5 \end{pmatrix} \quad \tau = \begin{pmatrix} 0 & 1 & 2 & 3 & 4 & 5 & 6 & 7 \\ 4 & 3 & 6 & 1 & 7 & 2 & 5 & 0 \end{pmatrix} \quad (4.3)$$

¹ In terms of the Feynman diagrams of the matrix model, σ and τ correspond to following either of the two lines of an edge in the direction of its (big) arrow.

or in terms of cycles $\sigma = (0\ 3\ 6)(1\ 4\ 2)(5\ 7)$ and $\tau = (0\ 4\ 7)(2\ 5\ 6)(1\ 3)$.

2) We are interested in *connected* maps. This amounts to requiring that the action on E of the group generated by σ and τ be transitive.

3) We mostly focus on diagrams without self-energy. In order to find self-energies (i.e. subdiagrams with 2 external legs), we look for pairs of edges (α, β) which belong to the same cycle of σ and to the same cycle of τ . Cutting these two edges amounts to composing with the transposition $(\alpha\beta)$: $\sigma' = \sigma \circ (\alpha\beta)$, $\tau' = \tau \circ (\alpha\beta)$. The diagram has no self-energy iff for all such pairs (α, β) , the modified diagram corresponding to (σ', τ') is still connected (note that in the planar case the resulting diagram is necessarily disconnected, so that the existence of such a pair is enough to discard the diagram).

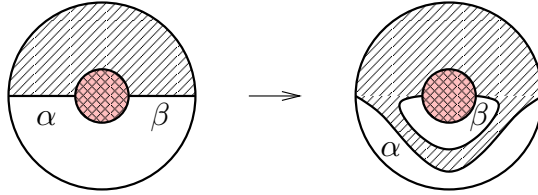


Fig. 14: Potential self-energies and how to cut them out.

4) Finally, we want to consider classes of flype-equivalent diagrams. The flype acts on a diagram as follows: consider four edges $(\alpha, \beta, \gamma, \delta)$ in the configuration depicted on Fig. 15a), that is $\sigma(\alpha) = \beta, \delta$ and γ in the same cycle of σ , α and δ, β and γ in the same cycles of τ . Cut the tangle by composing σ and τ with appropriate cycles, and paste its legs together in the way described on Fig. 15b). Proceed only if the resulting subdiagram is planar. If it is, then “flip” it by replacing σ and τ with their inverses inside it, see Fig. 15c). Finally, reconnect the tangle to the rest of the diagram, see Fig. 15d). A similar operation can be performed by exchanging black and white colors, i.e. σ and τ in the construction above. Together these two types of moves reproduce all possible flypes.

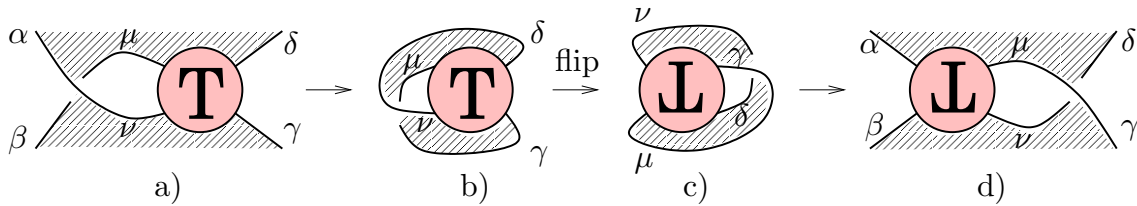


Fig. 15: Performing a flype via permutations.

4.2. Calculation of link invariants

There are various quantities one may want to compute once a permutation σ has been produced. They can be of many different types: first, they may be true invariants of virtual links, or they may be flype-invariant and therefore conjectured invariants of reduced alternating virtual link diagrams, or they may be not invariant at all (but still interesting to compute). Secondly, they may be invariants of *unoriented* or *oriented* links. In all that preceded we have only dealt with unoriented objects; however many useful invariants depend on orientation and it is therefore necessary to consider every choice of orientation (2^c where c is the number of connected components) of an unoriented object. We now list the quantities we have been able to compute, and how to extract them from the permutation σ :

(i) The number of crossings n is of course not left invariant by Reidemeister moves, but it is preserved by flypes. For reduced alternating diagrams of virtual links it is conjectured to be the minimal number of crossings.

(ii) The genus h of the underlying surface: it is *not* left invariant by general Reidemeister moves, as Fig. 16 shows (intuitively, after a Reidemeister move a handle may become empty so that it must be removed), however it is preserved by flypes, and once again, conjectured to be the minimal genus for virtual alternating links. It is given by the Euler–Poincaré formula: $\chi_E = 2 - 2h = \#V - \#E + \#F$, where $\#V = n$ is the number of vertices, $\#E = 2n$ is the number of edges, $\#F$ is the number of faces. If $\#\sigma$ is the number of cycles of σ i.e. of white faces, and similarly for τ , we have $\#F = \#\sigma + \#\tau$ and then we conclude that

$$h = 1 - \frac{1}{2}(\#\sigma + \#\tau - n) \tag{4.4}$$

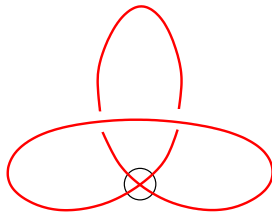


Fig. 16: A genus 1 diagram which turns out to be a trivial knot

(iii) The number of connected components c is of course an invariant of unoriented virtual links. Moving along each connected component on the diagram can be achieved by acting with ρ and $\tilde{\rho}$ alternately; it is easy to check that this implies

$$c = \frac{1}{2} \#(\rho\tilde{\rho}) = \frac{1}{2} \#(\sigma^{-2}\tau^2) \quad (4.5)$$

(iv) The order of symmetry of the diagram: this is not an invariant at all. It is simply the order of the group of permutations H that commute with both σ and τ , that is

$$H = \{g \in G \mid g\sigma = \sigma g\} . \quad (4.6)$$

This order is a divisor of $2n$ (this results from the fact that for tangles – see below – this group is trivial).

At low orders one can easily find pairs of flype-equivalent alternating reduced diagrams with distinct symmetry factors; this observation is important because it prevents us from computing the generating function of the number of prime alternating links in the same way as for tangles.

(v) The set of linking numbers: for an oriented diagram, define the sign ϵ_v of a vertex v according to Fig. 17, and

$$\ell_{ij} = \sum_{v \in V_{ij}} \epsilon_v \quad 1 \leq i, j \leq c \quad (4.7)$$

V_{ij} being the set of vertices where components labelled i and j meet.



Fig. 17: Sign of a vertex.

The off-diagonal elements ℓ_{ij} , $i < j$ are twice the usual linking numbers between components i and j (but they are not necessarily even for virtual diagrams). They are invariants of oriented links (up to permutation of the labels of the connected components). Their absolute value does not depend on orientation.

(vi) The determinant d is an invariant of unoriented links: it is a specialization of the usual Alexander polynomial (see below).

(vii) The bracket polynomial is defined for an unoriented diagram by a sum over “splittings”:

$$\langle L \rangle = \sum_s A^{a(s)-b(s)} (-A^2 - A^{-2})^{\#s-1} \quad (4.8)$$

where the splitting s is described at each vertex by Fig. 18; $a(s)$ and $b(s)$ are the number of vertices of type (a) and (b), and $\#s$ is the number of loops thus created.² Alternatively, s has a simple description as a permutation: define

$$s(i) = \begin{cases} \sigma(i) & \text{if } i \text{ overpasses a vertex of type (a)} \\ \tau(i) & \text{if } i \text{ overpasses a vertex of type (b)} \end{cases} \quad (4.9)$$

for all edges $i \in E$. Note that this induces an orientation of the loops (which is associated with the bicolouration of the faces). Then $\#s$ is the number of cycles of s .

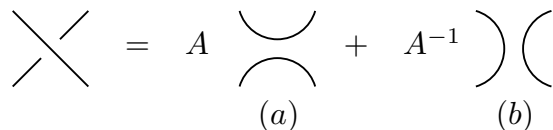


Fig. 18: Splitting at a vertex.

The bracket polynomial is preserved by flypes; however it is not invariant under Reidemeister move I. It is only up to multiplication by $-A$ that it is an invariant of unoriented links.

One can get rid of this arbitrary power of $-A$ by introducing

$$V = (-A)^{-3t} \langle L \rangle \quad (4.10)$$

where $t = \sum_{1 \leq i \leq c} \ell_{ii}$ is the twisting number of the link (which is orientation independent). V is (up to a power of A for multi-component links) the Jones polynomial in the variable $A = x^{1/4}$.

Furthermore, one can compute colored Jones polynomials by using cabling, i.e. replacing each string with k parallel strings and then adding extra “twists” to keep constant the linking number of each new string with the original one (e.g. keep it zero). We skip the details of the implementation; let us simply note that the computation time of the k -th

² It might seem surprising that loops that have non-trivial homology are not distinguished in Eq. (4.8); this is because homeomorphisms of Σ and addition/subtraction of handles do not preserve the homology class of loops.

cabling roughly grows like c_{2k}^n where $c_{2k} = \frac{(4k)!}{(2k)!(2k+1)!}$, so that only $k = 2$ can be achieved in a reasonable amount of time.

(viii) The Alexander polynomials are polynomial invariants of oriented links up to a sign and multiplication by a monomial. We refer to [18,19,1,20,21] for details. The (extended, multi-variable) Alexander module is defined by its generators, the edges of the diagram, and local linear relations at each vertex, see Fig. 19. They are very simple to build in terms of the permutation σ once an orientation has been fixed. The 0th polynomial (which vanishes for classical links) is simply the determinant of the matrix of relations. Further polynomial invariants are obtained as g.c.d. of minors.

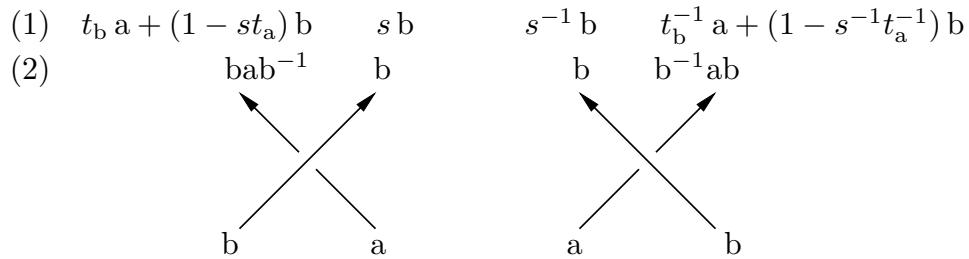


Fig. 19: The rules defining (1) the Alexander module and (2) the group of a link.

(ix) Closely related is the group π of a virtual link which is the generalization to virtual links of the fundamental group of the complement of a link; the relations at each vertex are described on Fig. 19. It is an invariant (up to isomorphism) of unoriented links (the orientation only fixes the presentation). In practice it is not a simple task (and not easy to implement by computer) to decide if two groups given by generators and relations are isomorphic, and one uses as invariants the number of morphisms of π into given finite groups Γ . Unfortunately this is only doable for Γ of small order, which only uncovers a small part of the structure of π .

4.3. Generalization to tangles

The appropriate way to consider a (four-legged) tangle is a link with a marked rigid vertex. All that has been done in sections 4.1 and 4.2 can therefore be adapted to the case of tangles.

A tangle is now represented by a pair of permutations (σ, τ) in which the marked vertex is encoded just like an ordinary crossing, except the labels must somehow determine uniquely which vertex is marked: in the implementation we chose the edges overcrossing

at the marked vertex to be $(2n - 2, 2n - 1)$. The actual tangle is obtained by removing the marked vertex and drawing the external legs in such a way that $2n - 2$ is the lower left line and $2n - 1$ is the upper right line (and therefore, $\sigma(2n - 1)$ is lower right and $\tau(2n - 1)$ is upper left).

The group of relabellings is now limited to those elements of g leaving the rigid vertex, i.e. the corresponding two labels $(2n - 2$ and $2n - 1)$, invariant: it is a subgroup G_1 of G which is isomorphic to $\mathcal{S}_{n-1} \times \mathbb{Z}_2^{n-1}$. Other operations on the permutations can be performed in the same spirit, that is by keeping the rigid vertex fixed.

Tangle invariants are generically obtained by pasting an arbitrary given tangle to the tangle under consideration and computing link invariants. In practice one obtains only a finite number of independent invariants. For example, one gets two Jones polynomials, and more generally c_{2k} for the k -cabling, by pasting arbitrary arch configurations to the tangle; five 0th Alexander polynomials obtained by setting equal to 0 two of the four generators corresponding to external legs and computing the resulting $(n - 1) \times (n - 1)$ determinant of the matrix of relations (there are $\binom{4}{2} = 6$ possibilities but only 5 are independent due to a bilinear identity satisfied by the determinants); etc.

4.4. Results

We have written a program that generates all permutations $\sigma \in \mathcal{S}_n$ up to conjugation by elements of G (or G_1 for tangles), for $n \leq 6$. It then selects connected prime/reduced diagrams, creates flype equivalence classes, and finally sorts them according to their invariants and in particular detects undistinguishable non flype-equivalent diagrams. We have provided a sample of the output on Fig. 20. In particular, the number of morphisms of the group π into the three groups S_3 , A_4 and A_5 is listed, but we have occasionally looked at higher groups. To save space, the variable A of the Jones polynomial is called a in the tables, and only 0th extended Alexander polynomials, depending on $c + 1$ variables t_0, \dots, t_{c-1} and s are listed. The rest can be found on the web (<http://ipnweb.in2p3.fr/~lptms/membres/pzinn/virtlinks>).

Up to order 4, we have checked that all flype-equivalence classes are distinguished by the invariants described in section 4.2. Therefore the conjecture holds true for links at least up to order 4.

When we go to higher orders, a new problem arises: the difficulty in distinguishing links obtained from one another by discrete symmetries.

c	d	morphisms S_3 A_4 A_5	Jones polynomial 2-cabled Jones polynomial	σ	σ mirror	s	h
ℓ			Alexander-Conway polynomials	0 1 2 3 4 5 6 7	0 1 2 3 4 5 6 7		
1	5	6 36 300	$+a^{-8} - a^{-4} + 1 - a^4 + a^8$ $-a^{-26} + a^{-22} - a^{-2} - a^2 + a^{22} - a^{26}$	3 4 1 6 2 7 0 5		2	0
2	4	30 72 1140	$-a^{-6} - a^{-2} + a^6 - a^{10}$ $-a^{-22} - a^{-14} - a^{-6} - a^{-2} - 2a^2 - a^{14} - a^{22} + a^{26} - a^{30}$	2 4 0 6 1 7 3 5	3 5 1 6 0 7 4 2	8	0
2	4	30 72 1140	$-a^{-10} + a^{-6} - a^{-2} - a^6$ $-a^{-30} + a^{-26} - a^{-22} - a^{-14} - 2a^{-2} - a^2 - a^6 - a^{14} - a^{22}$	3 5 1 6 0 7 4 2	2 4 0 6 1 7 3 5	8	0
1	5	6 12 180	$+a^4 + a^{12} - a^{16}$ $-a^2 - a^{10} + a^{14} - a^{18} - 3a^{22} - a^{26} + 3a^{30} + 4a^{34} - a^{38} - 2a^{42} - a^{46} + a^{50}$	3 5 1 6 2 7 4 0	2 4 0 6 3 7 1 5	4	1
1	5	6 12 180	$-a^{-16} + a^{-12} + a^{-4}$ $+a^{-50} - a^{-46} - 2a^{-42} - a^{-38} + 4a^{-34} + 3a^{-30} - a^{-26} - 3a^{-22} - a^{-18} + a^{-14} - a^{-10} - a^{-2}$	2 4 0 6 3 7 1 5	3 5 1 6 2 7 4 0	4	1
2	6	24 72 600	$-1 - a^4 - a^8 + a^{12}$ $-a^{-6} - 2a^{-2} - 2a^2 + 2a^6 - 4a^{10} - 8a^{14} + 6a^{18} + 6a^{22} - 3a^{26} - 3a^{30} + a^{38}$ $+1 - s^2 - 2st_0 + 2s^3t_0 - t_0t_1 + s^2t_0t_1 + s^2t_0^2 - s^4t_0^2 + 2st_0^2t_1 - 2s^3t_0^2t_1 - s^2t_0^3t_1 + s^4t_0^3t_1$	2 4 0 5 6 7 3 1	3 4 1 5 6 7 2 0	2	1
2	6	24 72 600	$+a^{-12} - a^{-8} - a^{-4} - 1$ $+a^{-38} - 3a^{-34} - 3a^{-30} + 6a^{-26} + 6a^{-22} - 8a^{-14} - 4a^{-10} + 2a^{-6} - 2a^{-2} - 2a^2 - a^6$ $+1 - s^2 - 2st_0 + 2s^3t_0 - t_0t_1 + s^2t_0t_1 + s^2t_0^2 - s^4t_0^2 + 2st_0^2t_1 - 2s^3t_0^2t_1 - s^2t_0^3t_1 + s^4t_0^3t_1$	3 4 1 5 6 7 2 0	2 4 0 5 6 7 3 1	2	1
2	6	24 72 600	$-2a^2 - a^{10} + a^{14}$ $+a^{-2} - 3a^2 - 6a^6 - 6a^{10} + 6a^{18} + a^{22} - a^{26} - a^{30} + a^{34} + a^{38} - a^{42}$ $+1 - s^2 - st_1 + s^3t_1 + s^2t_0t_1 - s^4t_0t_1 - t_0^2 + s^2t_0^2 + st_0^2 - s^3t_0^2 - s^2t_0^3t_1 + s^4t_0^3t_1$ $+1 - s^2 - st_0 + s^3t_0 - t_0t_1 + s^2t_0t_1 + s^2t_0^2 - s^4t_0^2 + st_0^2t_1 - s^3t_0^2t_1 - s^2t_0^3t_1 + s^4t_0^3t_1$ $+1 - s^2 - st_0 + s^3t_0 - t_0t_1 + s^2t_0t_1 + s^2t_0^2 - s^4t_0^2 + st_0^2t_1 - s^3t_0^2t_1 - s^2t_0^3t_1 + s^4t_0^3t_1$ $+1 - s^2 - st_1 + s^3t_1 + s^2t_0t_1 - s^4t_0t_1 - t_0^2 + s^2t_0^2 + st_0^2 - s^3t_0^2 - s^2t_0^3t_1 + s^4t_0^3t_1$	2 4 0 5 6 7 1 3	3 4 1 5 6 7 0 2	2	1
2	6	24 72 600	$+a^{-14} - a^{-10} - 2a^{-2}$ $-a^{-42} + a^{-38} + a^{-34} - a^{-30} - a^{-26} + a^{-22} + 6a^{-18} - 6a^{-10} - 6a^{-6} - 3a^{-2} + a^2$ $+1 - s^2 - st_1 + s^3t_1 + s^2t_0t_1 - s^4t_0t_1 - t_0^2 + s^2t_0^2 + st_0^2 - s^3t_0^2 - s^2t_0^3t_1 + s^4t_0^3t_1$ $+1 - s^2 - st_0 + s^3t_0 - t_0t_1 + s^2t_0t_1 + s^2t_0^2 - s^4t_0^2 + st_0^2t_1 - s^3t_0^2t_1 - s^2t_0^3t_1 + s^4t_0^3t_1$ $+1 - s^2 - st_0 + s^3t_0 - t_0t_1 + s^2t_0t_1 + s^2t_0^2 - s^4t_0^2 + st_0^2t_1 - s^3t_0^2t_1 - s^2t_0^3t_1 + s^4t_0^3t_1$ $+1 - s^2 - st_1 + s^3t_1 + s^2t_0t_1 - s^4t_0t_1 - t_0^2 + s^2t_0^2 + st_0^2 - s^3t_0^2 - s^2t_0^3t_1 + s^4t_0^3t_1$	3 4 1 5 6 7 0 2	2 4 0 5 6 7 1 3	2	1
4	8	162 768 12420	$-a^{-6} - 3a^{-2} - 3a^6 - a^6$ $-a^{-22} - 3a^{-18} - a^{-14} + 5a^{-10} - 18a^{-6} - 46a^{-2} - 46a^2 - 18a^6 + 5a^{10} - a^{14} - 3a^{18} - a^{22}$	2 3 4 5 6 7 0 1		8	1
1 0 1 1 0 1 -1 0 1 -1 0 1 -1 0 -1 1 0 1 1 0 -1 -1 0 1 1 0 -1 1 0 -1 -1 0 -1 -1 0 -1 -1 0 1 1 0 -1 1 0 1 -1 0 -1 1 0 1 -1 0 -1 -1 0 1 1 0 -1 -1 0 -1 -1 0 -1 1 0 -1 1 0 -1 1 0 -1 -1 0 1 -1 0 -1 1 0 1 -1 0 1 -1 0 1 1 0 1 1 0 1			$+1 - s^2 - st_3 + s^3t_3 - st_1 + s^3t_1 + s^2t_1t_3 - s^4t_1t_3 - t_0t_2 + s^2t_0t_2 + st_0t_2t_3 - s^3t_0t_2t_3 + st_0t_1t_2 - s^3t_0t_1t_2 - s^2t_0t_1t_2 + s^4t_0t_1t_2t_3$ $+1 - s^2 - st_2 + s^3t_2 - t_1t_3 + s^2t_1t_3 + st_1t_2t_3 - s^3t_1t_2t_3 - st_0 + s^3t_0 + s^2t_0t_2 - s^4t_0t_2 + st_0t_1t_3 - s^3t_0t_1t_3 - s^2t_0t_1t_2 + s^4t_0t_1t_2t_3$ $+1 - s^4 - st_3 + s^3t_3 - st_2 + s^3t_2 - st_1 + s^3t_1 + st_1t_2t_3 - s^3t_1t_2t_3 - st_0 + s^3t_0 + st_0t_2t_3 - s^3t_0t_2t_3 + st_0t_1t_3 - s^3t_0t_1t_3 + st_0t_1t_2 - s^2t_0t_1t_2 - t_0t_1t_2t_3 + s^4t_0t_1t_2t_3$ $+1 - s^2 - st_3 + s^3t_3 - st_1 + s^3t_1 + s^2t_1t_3 - s^4t_1t_3 - t_0t_2 + s^2t_0t_2 + st_0t_2t_3 - s^3t_0t_2t_3 + st_0t_1t_2 - s^3t_0t_1t_2 - s^2t_0t_1t_2 + s^4t_0t_1t_2t_3$ $+1 - s^4 - st_3 + s^3t_3 - st_2 + s^3t_2 - st_1 + s^3t_1 + st_1t_2t_3 - s^3t_1t_2t_3 - st_0 + s^3t_0 + st_0t_2t_3 - s^3t_0t_2t_3 + st_0t_1t_3 - s^3t_0t_1t_3 + st_0t_1t_2 - s^2t_0t_1t_2 - t_0t_1t_2t_3 + s^4t_0t_1t_2t_3$ $+1 - s^2 - st_2 + s^3t_2 - t_1t_3 + s^2t_1t_3 + st_1t_2t_3 - s^3t_1t_2t_3 - st_0 + s^3t_0 + s^2t_0t_2 - s^4t_0t_2 + st_0t_1t_3 - s^3t_0t_1t_3 - s^2t_0t_1t_2 + s^4t_0t_1t_2t_3$ $+1 - s^4 - st_3 + s^3t_3 - st_2 + s^3t_2 - st_1 + s^3t_1 + st_1t_2t_3 - s^3t_1t_2t_3 - st_0 + s^3t_0 + st_0t_2t_3 - s^3t_0t_2t_3 + st_0t_1t_3 - s^3t_0t_1t_3 + st_0t_1t_2 - s^2t_0t_1t_2 - t_0t_1t_2t_3 + s^4t_0t_1t_2t_3$ $+1 - s^2 - st_3 + s^3t_3 - st_1 + s^3t_1 + s^2t_1t_3 - s^4t_1t_3 - t_0t_2 + s^2t_0t_2 + st_0t_2t_3 - s^3t_0t_2t_3 + st_0t_1t_3 - s^3t_0t_1t_3 + st_0t_1t_2 - s^2t_0t_1t_2 - t_0t_1t_2t_3 + s^4t_0t_1t_2t_3$ $+1 - s^4 - st_3 + s^3t_3 - st_2 + s^3t_2 - st_1 + s^3t_1 + st_1t_2t_3 - s^3t_1t_2t_3 - st_0 + s^3t_0 + st_0t_2t_3 - s^3t_0t_2t_3 + st_0t_1t_3 - s^3t_0t_1t_3 + st_0t_1t_2 - s^2t_0t_1t_2 - t_0t_1t_2t_3 + s^4t_0t_1t_2t_3$ $+1 - s^2 - st_2 + s^3t_2 - t_1t_3 + s^2t_1t_3 + st_1t_2t_3 - s^3t_1t_2t_3 - st_0 + s^3t_0 + s^2t_0t_2 - s^4t_0t_2 + st_0t_1t_3 - s^3t_0t_1t_3 - s^2t_0t_1t_2 + s^4t_0t_1t_2t_3$ $+1 - s^2 - st_3 + s^3t_3 - st_1 + s^3t_1 + s^2t_1t_3 - s^4t_1t_3 - t_0t_2 + s^2t_0t_2 + st_0t_2t_3 - s^3t_0t_2t_3 + st_0t_1t_3 - s^3t_0t_1t_3 + st_0t_1t_2 - s^2t_0t_1t_2 - t_0t_1t_2t_3 + s^4t_0t_1t_2t_3$				
2	4	24 48 480	$-a^{-4} - a^4$ $+a^{-18} - a^{-14} - 2a^{-10} - 2a^{-6} - 2a^6 - 2a^{10} - a^{14} + a^{18}$	2 4 1 6 0 7 3 5	3 4 1 6 0 7 5 2	2	1
2	4	24 48 480	$-a^{-4} - a^4$ $+a^{-18} - a^{-14} - 2a^{-10} - 2a^{-6} - 2a^6 - 2a^{10} - a^{14} + a^{18}$	3 4 1 6 0 7 5 2	2 4 1 6 0 7 3 5	2	1

Fig. 20: Table of prime alternating links with 4 crossings. Mirror images are indicated only for chiral links. Only 0th (extended multi-variable) Alexander polynomials are listed.

c	d	morphisms S_3 A_4 A_5	Jones polynomial 2-cabled Jones polynomial	σ 0 1 2 3 4 5 6 7	σ mirror 0 1 2 3 4 5 6 7	s	h
Alexander-Conway polynomials							
ℓ							
2	6	24 48 360	$-a^{-4} - a^4$ $+a^{-18} - a^{-10} - 2a^{-6} - 2a^{-2} - 2a^2 - 2a^6 - a^{10} + a^{18}$	2 4 1 5 6 7 3 0		1	2
	-2 2 2 -2		$+1-s^2-st_1+s^3t_1-st_0+s^3t_0-t_0t_1+2s^2t_0t_1-s^4t_0t_1+2st_0t_1^2-2s^3t_0t_1^2-s^2t_0t_1^3+s^4t_0t_1^4$ $+1-s^2-2st_0+2s^3t_0-t_0^2+2s^2t_0^2-s^4t_0^2+st_0^2t_1-s^3t_0^2t_1+st_0^3-s^2t_0^3t_1+s^4t_0^3t_1$ $+1-s^2-st_1+s^3t_1-st_0+s^3t_0-t_0t_1+2s^2t_0t_1-s^4t_0t_1+2st_0t_1^2-2s^3t_0t_1^2-s^2t_0t_1^3+s^4t_0t_1^4$ $+1-s^2-2st_0+2s^3t_0-t_0^2+2s^2t_0^2-s^4t_0^2+st_0^2t_1-s^3t_0^2t_1+st_0^3-s^2t_0^3t_1+s^4t_0^3t_1$				
4	8	162 768 12420	$-3a^{-4} - 2 - 3a^4$ $+3a^{-18} - 2a^{-14} - 12a^{-10} - 24a^{-6} - 29a^{-2} - 29a^2 - 24a^6 - 12a^{10} - 2a^{14} + 3a^{18}$	2 3 4 5 6 7 1 0		8	2
	1 0 1 -1 0 1 -1 0 1 1 0 1 -1 0 -1 -1 0 1 1 0 -1 1 0 1 1 0 -1 -1 0 -1 -1 0 -1 1 0 -1 -1 0 -1 -1 0 -1 -1 0 1 1 0 -1 1 0 1 1 0 1 -1 0 1 -1 0 -1 -1 0 -1 -1 0 -1 1 0 -1 -1 0 -1 1 0 -1 1 0 1 -1 0 -1 -1 0 1 -1 0 1 1 0 1 1 0 1 -1 0 1		$+1-s^2-t_2t_3+s^2t_2t_3-st_1+s^3t_1+st_1t_2t_3-s^3t_1t_2t_3-st_0+s^3t_0+st_0t_2t_3-s^3t_0t_2t_3+s^2t_0t_1-t_1-s^4t_0t_1-s^2t_0t_1t_2t_3+s^4t_0t_1t_2t_3$ $+1-s^2-st_2+s^3t_2-st_1+s^3t_1+s^2t_1t_2-s^4t_1t_2-t_0t_3+s^2t_0t_3+st_0t_2t_3-s^3t_0t_2t_3+st_0t_1t_3-s^3t_0t_1t_3-s^2t_0t_1t_2t_3+s^4t_0t_1t_2t_3$ $+1-s^2-st_3+s^3t_3-t_1t_2+s^2t_1t_2+st_1t_2t_3-s^3t_1t_2t_3-st_0+s^3t_0+s^2t_0t_3-s^4t_0t_3+st_0t_1t_2-s^3t_0t_1t_2-s^2t_0t_1t_2t_3+s^4t_0t_1t_2t_3$ $+1-s^2-st_3+s^3t_3-st_2+s^3t_2+s^2t_2t_3-s^4t_2t_3-t_0t_1+s^2t_0t_1+st_0t_1t_3-s^3t_0t_1t_3+st_0t_1t_2-s^3t_0t_1t_2-s^2t_0t_1t_2t_3+s^4t_0t_1t_2t_3$ $+1-s^2-st_2+s^3t_2-st_1+s^3t_1+s^2t_1t_2-s^4t_1t_2-t_0t_3+s^2t_0t_3+st_0t_2t_3-s^3t_0t_2t_3+st_0t_1t_3-s^3t_0t_1t_3-s^2t_0t_1t_2t_3+s^4t_0t_1t_2t_3$ $+1-s^2-t_2t_3+s^2t_2t_3-st_1+s^3t_1+st_1t_2t_3-s^3t_1t_2t_3-st_0+s^3t_0+st_0t_2t_3-s^3t_0t_2t_3+s^2t_0t_1-t_1-s^4t_0t_1-s^2t_0t_1t_2t_3+s^4t_0t_1t_2t_3$ $+1-s^2-st_3+s^3t_3-st_2+s^3t_2+s^2t_2t_3-s^4t_2t_3-t_0t_1+s^2t_0t_1+st_0t_1t_3-s^3t_0t_1t_3+st_0t_1t_2-s^3t_0t_1t_2-s^2t_0t_1t_2t_3+s^4t_0t_1t_2t_3$ $+1-s^2-st_3+s^3t_3-t_1t_2+s^2t_1t_2+st_1t_2t_3-s^3t_1t_2t_3-st_0+s^3t_0+s^2t_0t_3-s^4t_0t_3+st_0t_1t_2-s^3t_0t_1t_2-s^2t_0t_1t_2t_3+s^4t_0t_1t_2t_3$ $+1-s^2-st_2+s^3t_2-st_1+s^3t_1+s^2t_1t_2-s^4t_1t_2-t_0t_3+s^2t_0t_3+st_0t_2t_3-s^3t_0t_2t_3+st_0t_1t_3-s^3t_0t_1t_3-s^2t_0t_1t_2t_3+s^4t_0t_1t_2t_3$ $+1-s^2-t_2t_3+s^2t_2t_3-st_1+s^3t_1+st_1t_2t_3-s^3t_1t_2t_3-st_0+s^3t_0+st_0t_2t_3-s^3t_0t_2t_3+s^2t_0t_1-t_1-s^4t_0t_1-s^2t_0t_1t_2t_3+s^4t_0t_1t_2t_3$ $+1-s^2-st_2+s^3t_2-st_1+s^3t_1+s^2t_1t_2-s^4t_1t_2-t_0t_3+s^2t_0t_3+st_0t_2t_3-s^3t_0t_2t_3+st_0t_1t_3-s^3t_0t_1t_3-s^2t_0t_1t_2t_3+s^4t_0t_1t_2t_3$ $+1-s^2-t_2t_3+s^2t_2t_3-st_1+s^3t_1+st_1t_2t_3-s^3t_1t_2t_3-st_0+s^3t_0+st_0t_2t_3-s^3t_0t_2t_3+s^2t_0t_1-t_1-s^4t_0t_1-s^2t_0t_1t_2t_3+s^4t_0t_1t_2t_3$ $+1-s^2-st_3+s^3t_3-st_2+s^3t_2+s^2t_2t_3-s^4t_2t_3-t_0t_1+s^2t_0t_1+st_0t_1t_3-s^3t_0t_1t_3+st_0t_1t_2-s^3t_0t_1t_2-s^2t_0t_1t_2t_3+s^4t_0t_1t_2t_3$ $+1-s^2-st_3+s^3t_3-t_1t_2+s^2t_1t_2+st_1t_2t_3-s^3t_1t_2t_3-st_0+s^3t_0+s^2t_0t_3-s^4t_0t_3+st_0t_1t_2-s^3t_0t_1t_2-s^2t_0t_1t_2t_3+s^4t_0t_1t_2t_3$ $+1-s^2-st_2+s^3t_2-st_1+s^3t_1+s^2t_1t_2-s^4t_1t_2-t_0t_3+s^2t_0t_3+st_0t_2t_3-s^3t_0t_2t_3+st_0t_1t_3-s^3t_0t_1t_3-s^2t_0t_1t_2t_3+s^4t_0t_1t_2t_3$ $+1-s^2-t_2t_3+s^2t_2t_3-st_1+s^3t_1+st_1t_2t_3-s^3t_1t_2t_3-st_0+s^3t_0+st_0t_2t_3-s^3t_0t_2t_3+s^2t_0t_1-t_1-s^4t_0t_1-s^2t_0t_1t_2t_3+s^4t_0t_1t_2t_3$ $+1-s^2-st_2+s^3t_2-st_1+s^3t_1+s^2t_1t_2-s^4t_1t_2-t_0t_3+s^2t_0t_3+st_0t_2t_3-s^3t_0t_2t_3+st_0t_1t_3-s^3t_0t_1t_3-s^2t_0t_1t_2t_3+s^4t_0t_1t_2t_3$ $+1-s^2-t_2t_3+s^2t_2t_3-st_1+s^3t_1+st_1t_2t_3-s^3t_1t_2t_3-st_0+s^3t_0+st_0t_2t_3-s^3t_0t_2t_3+s^2t_0t_1-t_1-s^4t_0t_1-s^2t_0t_1t_2t_3+s^4t_0t_1t_2t_3$				
2	4	18 48 300	$-a^{-2} - a^2$ $-a^{-18} + 3a^{-10} - 6a^{-2} - 6a^2 + 3a^{10} - a^{18}$	3 4 1 6 0 7 2 5		2	1
	0 0 0 0		0 $+1-s^2-st_1+s^3t_1-st_0+s^3t_0-t_0t_1+2s^2t_0t_1-s^4t_0t_1+st_0t_1^2-s^3t_0t_1^2+st_0t_1^3-s^2t_0t_1^3+s^4t_0t_1^4$ $+1-s^2-st_1+s^3t_1-st_0+s^3t_0-t_0t_1+2s^2t_0t_1-s^4t_0t_1+st_0t_1^2-s^3t_0t_1^2+st_0t_1^3-s^2t_0t_1^3+s^4t_0t_1^4$ 0				
2	4	30 72 1140	$-a^{-2} - a^2$ $-a^{-18} + 7a^{-10} - 10a^{-2} - 10a^2 + 7a^{10} - a^{18}$	2 4 1 6 0 7 5 3		4	1
	0 0 0 0		$+1-2s^2+s^4-2st_1+2s^3t_1-2st_0+2s^3t_0-2t_0t_1+4s^2t_0t_1-2s^4t_0t_1+2st_0t_1^2-2s^3t_0t_1^2+2st_0t_1^3-2s^2t_0t_1^3+s^4t_0t_1^4$ $+1-s^4-t_0^2t_1^2+s^4t_0^2t_1^2$ $+1-s^4-t_0^2t_1^2+s^4t_0^2t_1^2$ $+1-2s^2+s^4-2st_1+2s^3t_1-2st_0+2s^3t_0-2t_0t_1+4s^2t_0t_1-2s^4t_0t_1+2st_0t_1^2-2s^3t_0t_1^2+2st_0t_1^3-2s^2t_0t_1^3+s^4t_0t_1^4$				
2	6	24 48 360	$-a^{-2} - a^2$ $-2a^{-18} + 7a^{-10} + a^{-6} - 10a^{-2} - 10a^2 + a^6 + 7a^{10} - a^{18}$	2 4 1 5 6 7 0 3		1	1
	0 0 0 0		$+1-s^2-st_1+s^3t_1-2st_0+2s^3t_0+s^2t_0t_1-s^4t_0t_1-t_0^2+s^2t_0^2+2st_0t_1-2s^3t_0t_1+st_0^3-s^2t_0^3t_1+s^4t_0^3t_1$ $+1-s^2-st_1+s^3t_1-2st_0+2s^3t_0+s^2t_0t_1-s^4t_0t_1-t_0^2+s^2t_0^2+2st_0t_1-2s^3t_0t_1+st_0^3-s^2t_0^3t_1+s^4t_0^3t_1$ $+1-s^2-st_1+s^3t_1-2st_0+2s^3t_0+s^2t_0t_1-s^4t_0t_1-t_0^2+s^2t_0^2+2st_0t_1-2s^3t_0t_1+st_0^3-s^2t_0^3t_1+s^4t_0^3t_1$ $+1-s^2-st_1+s^3t_1-2st_0+2s^3t_0+s^2t_0t_1-s^4t_0t_1-t_0^2+s^2t_0^2+2st_0t_1-2s^3t_0t_1+st_0^3-s^2t_0^3t_1+s^4t_0^3t_1$				
1	5	6 12 180	$+1$ $+a^{-6} - 2a^{-2} - 3a^2 + 2a^6 + 2a^{10} - a^{14} - 3a^{18} + 3a^{26} - a^{34}$	3 4 1 6 2 7 5 0	2 4 1 6 3 7 0 5	1	1
			$+1-s^2-st+s^3t-t^2+s^2t^2+st^3-s^3t^3$ $+1-s^2-st+s^3t-t^2+s^2t^2+st^3-s^3t^3$				
1	5	6 12 180	$+1$ $+a^{-14} + 2a^{-10} - 4a^{-2} - 4a^2 + 2a^{10} + a^{14}$	2 4 1 6 3 7 5 0		1	2
			$+1-s^2-2st+2s^3t-t^2+2s^2t^2-s^4t^2+2st^3-2s^3t^3-s^2t^4+s^4t^4$ $+1-s^2-2st+2s^3t-t^2+2s^2t^2-s^4t^2+2st^3-2s^3t^3-s^2t^4+s^4t^4$				
1	5	6 12 180	$+1$ $-a^{-34} + 3a^{-26} - 3a^{-18} - a^{-14} + 2a^{-10} + 2a^{-6} - 3a^{-2} - 2a^2 + a^6$	2 4 1 6 3 7 0 5	3 4 1 6 2 7 5 0	1	1
			$+1-s^2-st+s^3t-t^2+s^2t^2+st^3-s^3t^3$ $+1-s^2-st+s^3t-t^2+s^2t^2+st^3-s^3t^3$				

Fig. 20 (continued)

Several discrete operations may be performed within the class of alternating virtual link diagrams. First, there is the mirror symmetry, a reflection in a plane orthogonal to the plane of the figure. This is a well known operation on classical knots and links, which are called achiral or chiral depending on whether the mirror image is equivalent or not to the original. The same applies to virtual diagrams. In terms of permutations it corresponds to $\sigma \leftrightarrow \tau$. Secondly, there is the simultaneous change of all over- into under-crossings and vice versa (which corresponds to $\sigma \rightarrow \tau^{-1}$, $\tau \rightarrow \sigma^{-1}$). For classical links, this is not independent of the mirror symmetry, as the composition of the two ($\sigma \rightarrow \sigma^{-1}$, $\tau \rightarrow \tau^{-1}$), which is equivalent to a global flip of the diagram, i.e. a rotation around an axis in the plane of the figure, yields a link equivalent to the original: this may be seen by gradually

overturning the link diagram. For virtual diagrams, this is no longer the case: there is an obstruction to this overturning due to the virtual crossings, and the impossibility of performing the “forbidden Reidemeister move” of Fig. 4. Accordingly, there are now some virtual links that are equivalent to their flip, and some that are not, the latter appearing at order 5, see for example Fig. 21.

In principle, mirror symmetry can be detected by the Jones polynomial since it corresponds to the transformation $A \rightarrow A^{-1}$. In fact, even the usual Alexander–Conway polynomial can distinguish mirror symmetric links in higher genus, since it is no longer reciprocal. It is important to notice that unlike classical alternating links, virtual alternating links do not necessarily saturate the bounds on minimum and maximum degrees of their Jones polynomial (maximum degree minus minimum degree in A^4 is less than or equal to $n - h$). For example, there are many virtual alternating links with trivial Jones polynomial. Therefore even detection of mirror symmetry can be tricky in higher genus. The situation is worse for the flip symmetry since the Jones polynomial (and cabled Jones polynomials) cannot distinguish flipped images at all. The group of the link or the higher Alexander–Conway polynomials may in some cases distinguish them.

In practice, already at order 5 there are several diagrams which are not related by flypes to their flips but for which we have not found any invariants to distinguish them. This is the case for four pairs of links with five crossings, namely those of Fig. 22 and 23 and their mirror images. At order 6, there are cases of undistinguishable flips and of undistinguishable mirror images. Based on the experience at genus 0, we believe that these issues are probably difficult to resolve and leave them to future work.

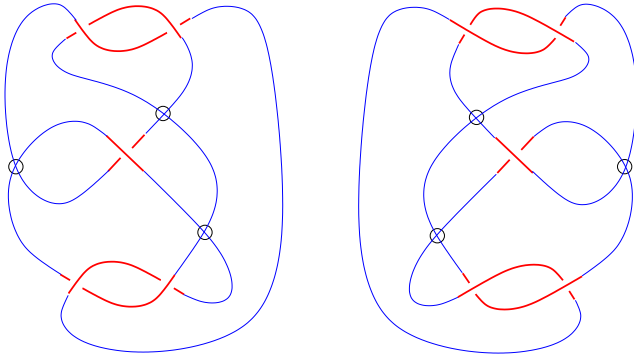


Fig. 21: A pair of virtual flipped knots, distinguished by their Alexander–Conway polynomial.

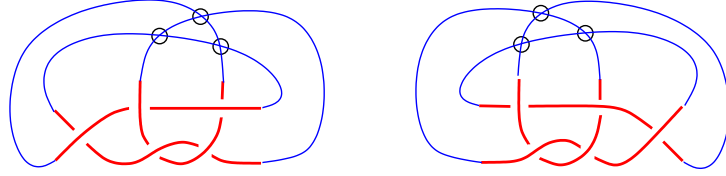


Fig. 22: A pair of virtual flipped knots of genus 1, conjectured to be non equivalent.

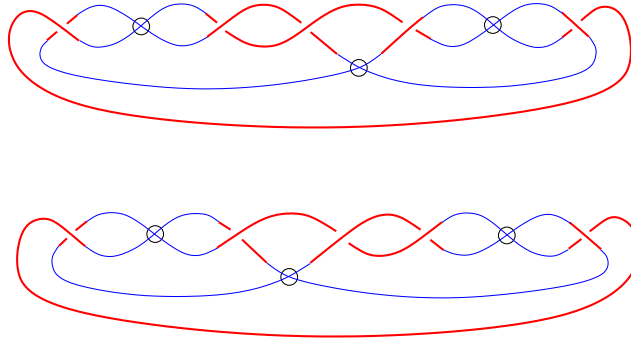


Fig. 23: A pair of virtual flipped knots of genus 2, conjectured to be non equivalent.

Let us now discuss the case of tangles, which is in fact more important for us since it is the objects which we enumerate. Fortunately the rigid vertex destroys any possible symmetries and the classification problem becomes easier. Fig. 24 shows a very limited sample of our data.

We have compared the 13010 virtual prime reduced alternating tangle diagrams up to order 5. We have performed the flype equivalence and checked that the number of tangles of each genus agrees with Eq. (3.10). Our program then allows us to assert that all the flype-equivalence classes thus obtained, irrespective of genus and crossing number, are distinct (note that in a few cases we had to manually feed the computer groups of fairly large order – up to 432 – to make it distinguish the corresponding link groups via their morphisms). This we consider a strong argument in favor of our generalized flype conjecture.

Acknowledgments

It is a pleasure to thank L. Funar, L. Kauffman, G. Kuperberg, P. Vogel for discussions, and G. Akemann for providing us with unpublished data by P. Adamietz and himself. J.-B. Z. is partially supported by the European network HPRN-CT-2002-00325.

t	c	d	morphisms $S_3 A_4 A_5$	Jones polynomials	σ 0 1 2 3 4 5	h	
Alexander-Conway polynomials							
1	3	4 0 2 2 2 2	108 576 18000	$\frac{-a^{-3}-a^1}{-a^{-3}-a^5}$	2 3 4 5 0 1	1	
0 1 -1		$+1-st_2-st_1+s^2t_1t_2$	0	$+s-t_0$	$+s-t_0$	$+s-t_0$	$+s-t_0$
0 -1 -1		$+1-st_2-st_1+s^2t_1t_2$	0	$+1-st_0$	$+1-st_0$	$+1-st_0$	$+1-st_0$
0 1 1		$+1-st_2-st_1+s^2t_1t_2$	0	$+1-st_0$	$+1-st_0$	$+1-st_0$	$+1-st_0$
0 -1 1		$+1-st_2-st_1+s^2t_1t_2$	0	$+s-t_0$	$+s-t_0$	$+s-t_0$	$+s-t_0$
0 -1 1		$+1-st_2-st_1+s^2t_1t_2$	0	$+s-t_0$	$+s-t_0$	$+s-t_0$	$+s-t_0$
0 1 1		$+1-st_2-st_1+s^2t_1t_2$	0	$+1-st_0$	$+1-st_0$	$+1-st_0$	$+1-st_0$
0 -1 -1		$+1-st_2-st_1+s^2t_1t_2$	0	$+1-st_0$	$+1-st_0$	$+1-st_0$	$+1-st_0$
0 1 -1		$+1-st_2-st_1+s^2t_1t_2$	0	$+s-t_0$	$+s-t_0$	$+s-t_0$	$+s-t_0$
1	3	4 0 2 2 2 2	108 576 18000	$\frac{-a^{-5}-a^3}{-a^{-1}-a^3}$	2 3 4 5 1 0	1	
0 -1 -1		$+1-st_2-st_1+s^2t_1t_2$	0	$+1-st_0$	$+1-st_0$	$+1-st_0$	$+1-st_0$
0 1 -1		$+1-st_2-st_1+s^2t_1t_2$	0	$+s-t_0$	$+s-t_0$	$+s-t_0$	$+s-t_0$
0 -1 1		$+1-st_2-st_1+s^2t_1t_2$	0	$+s-t_0$	$+s-t_0$	$+s-t_0$	$+s-t_0$
0 1 1		$+1-st_2-st_1+s^2t_1t_2$	0	$+1-st_0$	$+1-st_0$	$+1-st_0$	$+1-st_0$
0 1 1		$+1-st_2-st_1+s^2t_1t_2$	0	$+1-st_0$	$+1-st_0$	$+1-st_0$	$+1-st_0$
0 -1 1		$+1-st_2-st_1+s^2t_1t_2$	0	$+s-t_0$	$+s-t_0$	$+s-t_0$	$+s-t_0$
0 1 -1		$+1-st_2-st_1+s^2t_1t_2$	0	$+s-t_0$	$+s-t_0$	$+s-t_0$	$+s-t_0$
0 -1 -1		$+1-st_2-st_1+s^2t_1t_2$	0	$+1-st_0$	$+1-st_0$	$+1-st_0$	$+1-st_0$
2	2	3 1 1 1 2 2	36 144 3600	$\frac{+a^5}{-a^{-3}-a^5}$	2 4 0 5 3 1	1	
2		$+1-st_1-st_0$	+1	+1	+1	$+1-st_0$	$+1-st_1$
-2		$+1-st_0+s^2t_0t_1$	+1	+1	+1	$+1-st_0$	$+1-st_1$
-2		$+1-st_1+s^2t_0t_1$	+1	+1	+1	$+1-st_0$	$+1-st_1$
2		$+t_1+t_0-st_0t_1$	+1	+1	+1	$+1-st_0$	$+1-st_1$
2	2	3 1 1 1 2 2	36 144 3600	$\frac{+a^{-1}}{-a^{-1}-a^3}$	2 4 1 5 3 0	1	
0		$+1-st_0+s^2t_0t_1$	+1	+1	+1	$+1-st_0$	$+1-st_1$
0		$+1-st_1-st_0-t_0t_1+s^2t_0t_1$	+1	+1	+1	$+1-st_0$	$+1-st_1$
0		$+1-s^2-st_1-st_0+s^2t_0t_1$	+1	+1	+1	$+1-st_0$	$+1-st_1$
0		$+1-st_1+s^2t_0t_1$	+1	+1	+1	$+1-st_0$	$+1-st_1$
2	2	3 1 1 1 2 2	36 144 3600	$\frac{+a^{-1}}{-a^{-1}-a^3}$	3 4 0 5 2 1	1	
0		$+1-st_1+s^2t_0t_1$	+1	+1	+1	$+1-st_0$	$+1-st_1$
0		$+1-s^2-st_1-st_0+s^2t_0t_1$	+1	+1	+1	$+1-st_0$	$+1-st_1$
0		$+1-st_1-st_0-t_0t_1+s^2t_0t_1$	+1	+1	+1	$+1-st_0$	$+1-st_1$
0		$+1-st_0+s^2t_0t_1$	+1	+1	+1	$+1-st_0$	$+1-st_1$
2	2	3 1 1 1 2 2	36 144 3600	$\frac{+a^{-7}}{-a^{-3}-a^5}$	3 4 1 5 2 0	0	
-2		$+t_1+t_0-st_0t_1$	+1	+1	+1	$+1-st_0$	$+1-st_1$
2		$+1-st_1+s^2t_0t_1$	+1	+1	+1	$+1-st_0$	$+1-st_1$
2		$+1-st_0+s^2t_0t_1$	+1	+1	+1	$+1-st_0$	$+1-st_1$
-2		$+1-st_1-st_0$	+1	+1	+1	$+1-st_0$	$+1-st_1$
3	2	3 1 2 2 1 1	36 144 3600	$\frac{-a^{-5}-a^3}{+a^7}$	2 4 0 5 1 3	0	
2		$+1-st_1-st_0$	+1	$+1-st_1$	$+1-st_0$	+1	+1
-2		$+1-st_0+s^2t_0t_1$	+1	$+1-st_1$	$+1-st_0$	+1	+1
-2		$+1-st_1+s^2t_0t_1$	+1	$+1-st_1$	$+1-st_0$	+1	+1
2		$+t_1+t_0-st_0t_1$	+1	$+1-st_1$	$+1-st_0$	+1	+1
3	2	3 1 2 2 1 1	36 144 3600	$\frac{-a^{-3}-a^1}{+a^1}$	3 4 0 5 1 2	1	
0		$+1-st_0+s^2t_0t_1$	+1	$+1-st_1$	$+1-st_0$	+1	+1
0		$+1-st_1-st_0-t_0t_1+s^2t_0t_1$	+1	$+1-st_1$	$+1-st_0$	+1	+1
0		$+1-s^2-st_1-st_0+s^2t_0t_1$	+1	$+1-st_1$	$+1-st_0$	+1	+1
0		$+1-st_1+s^2t_0t_1$	+1	$+1-st_1$	$+1-st_0$	+1	+1
3	2	3 1 2 2 1 1	36 144 3600	$\frac{-a^{-3}-a^1}{+a^1}$	2 4 1 5 0 3	1	
0		$+1-st_1+s^2t_0t_1$	+1	$+1-st_1$	$+1-st_0$	+1	+1
0		$+1-s^2-st_1-st_0+s^2t_0t_1$	+1	$+1-st_1$	$+1-st_0$	+1	+1
0		$+1-st_1-st_0-t_0t_1+s^2t_0t_1$	+1	$+1-st_1$	$+1-st_0$	+1	+1
0		$+1-st_0+s^2t_0t_1$	+1	$+1-st_1$	$+1-st_0$	+1	+1
3	2	3 1 2 2 1 1	36 144 3600	$\frac{-a^{-5}-a^3}{+a^{-5}}$	3 4 1 5 0 2	1	
-2		$+t_1+t_0-st_0t_1$	+1	$+1-st_1$	$+1-st_0$	+1	+1
2		$+1-st_1+s^2t_0t_1$	+1	$+1-st_1$	$+1-st_0$	+1	+1
2		$+1-st_0+s^2t_0t_1$	+1	$+1-st_1$	$+1-st_0$	+1	+1
-2		$+1-st_1-st_0$	+1	$+1-st_1$	$+1-st_0$	+1	+1

Fig. 24: Table of prime alternating tangles with 2 crossings. t is the type of the tangles which encodes how external legs are connected to each other, according to: NW connected to $t = 1$ SE, $t = 2$ NE, $t = 3$ SW.

References

- [1] L. Kauffman, *Virtual knot theory*, *Europ. J. Combin.* **20** (1999) 663-690, [math.GT/9811028](#); *Detecting virtual knots*, Chicago preprint.
- [2] G. Kuperberg, *What is a virtual link?*, [math.GT/0208039](#).
- [3] W.W. Menasco and M.B. Thistlethwaite, *The Tait Flyping Conjecture*, *Bull. Amer. Math. Soc.* **25** (1991) 403–412; *The Classification of Alternating Links*, *Ann. Math.* **138** (1993) 113–171.
- [4] P. Zinn-Justin and J.-B. Zuber, *Matrix integrals and the counting of tangles and links*, *Discr. Math.* **246** (2002) 343-360, [math-ph/9904019](#).
- [5] P. Zinn-Justin, *The General $O(n)$ Quartic Matrix Model and its application to Counting Tangles and Links*, [math-ph/0106005](#).
- [6] C. Sundberg and M. Thistlethwaite, *The rate of Growth of the Number of Prime Alternating Links and Tangles*, *Pac. J. Math.* **182** (1998) 329–358.
- [7] G. 't Hooft, *A Planar Diagram Theory for Strong Interactions*, *Nucl. Phys.* **B 72** (1974) 461–473.
- [8] T.R. Morris, *Chequered surfaces and complex matrices*, *Nucl. Phys.* **B 356** (1991) 703-728.
- [9] G. Akemann, unpublished notes, private communication.
- [10] P. Adamietz, *Kollektive Feldtheorie und Momentenmethode in Matrixmodellen*, PhD thesis, internal report DESY T-97-01.
- [11] J. Ambjørn, C.F. Kristjansen, Y.M. Makeenko, *Higher Genus Correlators for the Complex Matrix Model*, *Mod.Phys.Lett.* **A7** (1992) 3187-3202, [hep-th/9207020](#).
- [12] S. Kunz-Jacques and G. Schaeffer, *The asymptotic number of prime alternating links*, Proceedings of the 14th international conference on Formal Power Series and Algebraic Combinatorics, Phenix, 2001.
- [13] D. Bessis, C. Itzykson and J.-B. Zuber, *Quantum Field Theory Techniques in Graphical Enumeration*, *Adv. Appl. Math.* **1** (1980) 109–157.
- [14] M. Bousquet-Mélou and G. Schaeffer, *Enumeration of planar constellations*, *Adv. in Appl. Math.* 24(4) (2000) 337–368;
G. Schaeffer, *Conjugaison d'arbres et cartes combinatoires aléatoires*, Thèse de doctorat, <http://dept-info.labri.u-bordeaux.fr/~schaeffe/cv/bibli/These.html>
- [15] B. Collins, *Moments and cumulants of polynomial random variables on unitary groups, the Itzykson-Zuber integral and free probability*, [math-ph/0205010](#), *Int.Math.Res.Notices*, to appear.
- [16] A. Zvonkin, *Matrix Integrals and Map Enumeration: An Accessible Introduction*, *Math. Comp. Modelling* **26** (1997) 281–304.
- [17] P. Di Francesco, P. Ginsparg and J. Zinn-Justin, *2D Gravity and Random Matrices*, *Phys. Rep.* **254** (1995) 1–133, [hep-th/9306153](#).

- [18] D.S. Silver and S.G. Williams, *Alexander groups and virtual links*, *J. Knot Theory and its Ramifications* to appear.
- [19] J. Sawollek, *On Alexander–Conway polynomials for virtual knots and links*, [math.GT/9912173](https://arxiv.org/abs/math/9912173).
- [20] L. Kauffman and D.E. Radford, *Bioriented Quantum Algebras, and a Generalized Alexander Polynomial for Virtual Links*, <http://www.math.uic.edu/~kauffman/Papers.html>
- [21] A. Bartholomew and R. Fenn, *Quaternionic Invariants of Virtual Knots and Links*, preprint.

Appendix A. Computation of the lowest order term of genus h

According to the description of the g expansion in terms of permutations of S_{2n} , the leading term with $n = 2h$ reads

$$F_{2h}^{(h)} = \frac{1}{(2n-1)!!} \frac{1}{2^n n!} \sum_{\sigma, \tau \in S_{2n}} \delta_{[\sigma], \{2n\}} \delta_{[\tau], \{2n\}} \delta_{[\sigma^{-1}\tau], \{2n\}} \quad (\text{A.1})$$

where the factor $\frac{1}{2^n n!}$ comes from the n -th order of the g expansion, and $\frac{1}{(2n-1)!!}$ takes care of the remaining relabeling invariance of the permutations. Also $[\sigma]$ denotes the class of the permutation σ . One then uses the orthonormalized characters of the S_{2n} symmetric group to represent the conditions on σ or τ by $\delta_{[\sigma], \{\alpha\}} = \sum_Y \frac{\nu_\alpha}{(2n)!} \chi_Y(\alpha) \chi_Y([\sigma])$ where the sum runs over Young tableaux with $2n$ boxes, and ν_α is the number of elements of the class α : if $\alpha = \{1^{\alpha_1} 2^{\alpha_2} \dots\}$, $\nu_\alpha = (2n)! / \prod_j (\alpha_j! j^{\alpha_j})$. Thus

$$\begin{aligned} (4h)! F_{2h}^{(h)} &= \sum_{\sigma, \tau \in S_{4h}} \left(\frac{\nu_{\{4h\}}}{(4h)!} \right)^2 \left(\frac{\nu_{\{2^{2h}\}}}{(4h)!} \right) \\ &\quad \times \sum_{Y_1, Y_2, Y_3} \chi_{Y_1}([\sigma]) \chi_{Y_1}(\{4h\}) \chi_{Y_2}([\tau]) \chi_{Y_2}(\{4h\}) \chi_{Y_3}([\sigma^{-1}\tau]) \chi_{Y_1}(\{2^{2h}\}) \\ &= \frac{\nu_{\{4h\}}^2 \nu_{\{2^{2h}\}}}{(4h)!} \sum_Y \frac{1}{d_Y} (\chi_Y(\{4h\}))^2 \chi_Y(\{2^{2h}\}) . \end{aligned} \quad (\text{A.2})$$

The characters $\chi_Y(\{2n\})$ for the one-cycle class receive contributions only from the hook

Young tableaux $Y_s = \overbrace{\begin{array}{|c|c|c|c|c|c|c|c|c|c|} \hline \square & \square & \square & \square & \square & \square & \square & \square & \square & \square \\ \hline \square & & & & & & & & & \\ \hline \square & & & & & & & & & \\ \hline \square & & & & & & & & & \\ \hline \end{array}}^{2n-s}$ for which

$$\begin{aligned} \chi_{Y_s}(\{2n\}) &= (-1)^s, \\ \chi_{Y_s}(\{2^n\}) &= (-1)^{\lfloor \frac{s+1}{2} \rfloor} \binom{n-1}{\lfloor \frac{s}{2} \rfloor} \\ d_{Y_s} &= \frac{(2n-1)!}{s!(2n-s-1)!} . \end{aligned}$$

The summation in (A.2) is thus reduced to a sum over $s = 0, \dots, 4h-1$. After some algebra, one finds the result (1.6).

The first subleading term $F_{2h+1}^{(h)}$ is given in a similar way by

$$F_{2h+1}^{(h)} = \frac{1}{(2n-1)!!} \frac{2}{2^n n!} \sum_{\sigma, \tau \in S_{2n}} \sum_{p=1}^n \delta_{[\sigma], \{2n\}} \delta_{[\tau], \{p, 2n-p\}} \delta_{[\sigma^{-1}\tau], \{2n\}} \quad (\text{A.3})$$

with now $n = 2h + 1$, since $F = 3$ implies that either $\#\sigma = 1$, $\#\tau = 2$ or the converse. The same method as above applies, again only hook Young tableaux contribute, and the only additional piece of information required is

$$\chi_{Y_s}(\{2n - p, p\}) = \begin{cases} (-1)^s & \text{if } s + 1 \leq p \leq 2n - s - 1, \\ (-1)^{s+1} & \text{if } 2n - s \leq p \leq s \\ 0 & \text{otherwise} \end{cases},$$

as we learn from the Murnaghan-Natayama formula. A little algebra then leads to the result (1.7).